Irrigation Performance Assessment using SEBS and SCOPE.
A case study of Tons pump Canal Command in India.

DERRICK MARIO DENIS
[February, 2013]

SUPERVISORS:
Dr. Ir. J Timmermans
Ir. G.N. Parodi

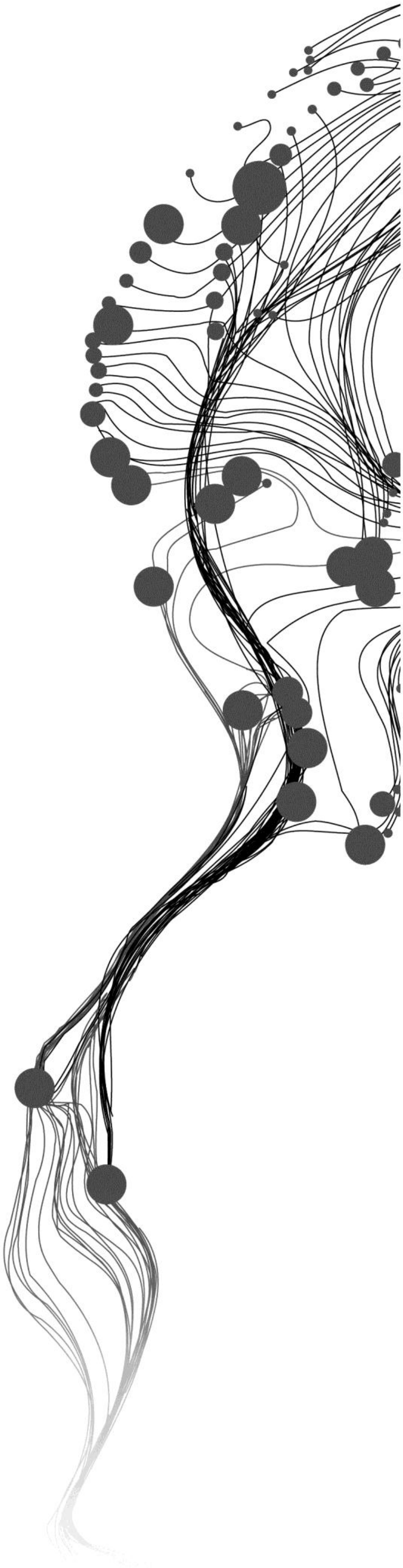

Irrigation Performance Assessment using SEBS and SCOPE. A case study of Tons pump Canal Command in India.

DERRICK MARIO DENIS

Enschede, The Netherlands, February,2013

Thesis submitted to the Faculty of Geo-Information Science and Earth Observation of the University of Twente in partial fulfilment of the requirements for the degree of Master of Science in Geo-information Science and Earth Observation.
Specialization: Water Resource and Environmental Management

SUPERVISORS:
Dr. Ir. Joris. Timmermans
Ir. Gabriel. N. Parodi

THESIS ASSESSMENT BOARD:
Dr. Ir. M.W.(Maciek) Lubczynski (Chair)
Dr. Ir. J.G.P.W. Clevers (External Examiner, Wageningen University)

To

my family

especially

Niharika,
Emmanuel and Aditi.

ABSTRACT

Evapotranspiration (ET) is the second largest component of the terrestrial water budget after precipitation. In semi-arid regions about ninety percent of annual precipitation is consumed in ET. Accurate estimates of ET are required for efficient management tasks from local to regional scales, such as irrigation water management. The use of several existing algorithms for estimation of ET from remotely sensed images is now a proven fact. Recent advances in remote sensing tools and the increase in computational power coupled with the availability of open source remotely sensed data is encouraging. Researchers are developing methodologies to quantify uncertainties while efforts are made to enhance its resolution and accuracy. However, the issue of quantification of uncertainties from discrepancy between earth observation resolutions and plot sizes remains.

Comparison between low resolution evapotranspiration and field measurement always have large uncertainties. This is mainly caused due to scale issues. It can be reduced by developing techniques to upscale them to high resolutions. Cost effective methods to develop this techniques on a spatial and temporal scales must be devised, especially when an irrigated area has to be assessed. This helps the user to improve the management of an irrigated area.

In this research the daily ET estimates for wheat grown on an irrigated area in the northern plains of India, is obtained through Surface Energy Balance System (SEBS) combining low resolution MODIS data along with meteorological information. This ET is disaggregated to obtain high resolution ET estimates for wheat by taking into account the variability in land cover over the irrigated area. The results are compared against a Soil Vegetation Atmosphere Transfer (SVAT) model for two crop growing periods for the years 2010-11 and 2011-12. For this purpose the Soil Canopy Observation, Photochemistry and Energy fluxes (SCOPE) model is also used to simulate the latent heat dynamics, to determine the ET for the wheat crop. These results are compared for two, crop growing seasons: 2010-11 and 2011-12.

The results revealed that the methodology used to enhance resolution and accuracy (upscaling), increases the correlation between SCOPE and SEBS estimates from 0.34 to 0.49 for the year 2010-11. The upscaled high resolution ETa is used to evaluate an irrigated area. The water balance indicators reveal that the present water supply is far less than adequate. The method developed successfully assesses an irrigated area.

Keywords : Evapotranspiration, upscaling, SEBS, SCOPE, MODIS

ACKNOWLEDGEMENTS

An opportunity to write an acknowledgement for Master's after a Ph.D. is rare. The answer to the burning question of "what next" kept haunting me. Indeed it was Europe. The long spells spent here in isolation away from my loved ones, did not go in vain for God revealed HIS love for me and it was '*awesome*'. All glory and honour be to my Lord and God, Jesus, for yet another opportunity to thank and praise HIS Holy Name.

I would like to take this opportunity to thank my Guru Rt. Rev. Prof Dr R.B.lal., H'ble Vice Chancellor, SamHiggon Bottom Institute of Agriculture, Technology and Sciences- Deemed University, for his kind permission and guidance towards me perusing studies at the ITC.

I am extremely thankful to my supervisor Dr. Ir. Joris, Researcher, Dept. of Water Resources, for his intelligent guidance and patience to guide me during this research. His ideas of writing a thesis have helped me to a great extent in improving my writing skills. I am also thankful to my second supervisor Ir. Gabriel, Lecturer, Dept. of Water Resources, for help received during the writing of the proposal and several suggestions for orienting this research in the right direction. His suggestions and remarks have enhanced the quality of this research. Special thanks are due to Dr Christiaan, Assistant Professor, Dept. of Water Resources, for his guidance in understanding and executing SCOPE successfully. I am thankful to all my teachers who taught me several courses at the ITC especially Dr. Tom Rientjes. I am also thankful to Prof Z Su, Head, Dept. of Water Resources for extending a warm welcome and hospitality to my H'ble Vice Chancellor during his visit to the ITC. Special thanks are due to Ir. Lieshout, Course Director WREM, for his support and help received during my study.

Special thanks are due to the farmers of the Samrakalwana village (study area), Allahabad, my colleagues Santosh, Avanish, Navneet, Mukesh, Rakesh ji, Ashish Rai and all who helped in the data collection. I do acknowledge my Dept. for providing me with the field data .The encouragement and help received from Rahul Raj, Ahmad Esa(Egypt), Mr Edward(Indonesia) and my classmates Zemede, Assama, Tsi Tsi, Melaku, Habte, Juliana, Ahmad, Mariam, Sabah, Ruta and Wossenu will always be appreciated. I will also like to appreciate the warm greeting I always received by Dr. Paul and Mrs Mieka and family, Bro. Jan and family and especially my Brother in Law Dr. J. A. Lal his wife Mrs Abhilasha and family. I was always at home with them. Sundays at the ITC hotel were special with the Sunday service at the International Christian Fellowship. I appreciate the opportunity giving me a chance to preach and that too for Christmas.

I will also like to mention in a special way the encouragements received by my parents, in laws, brothers and sisters during my stay in the Netherlands. Indeed the time was long but your prayers always made me feel one with the family. No words can thank the encouragement and support I received from my wife Niharika. It was her 'YES' that I could make it to the ITC. The patience of my son Emmanuel and the longing of my daughter Aditi can never be compensated. I felt it every day and I missed you every moment of it.

With great gratitude, I do acknowledge the scholarship received by the World Bank for this M.Sc. The data received from the sites of NASA and ECMWF are acknowledged.

Derrick Mario Denis.

TABLE OF CONTENTS

LIST OF SYMBOLS

E^{-}	Externally generated fluxes	$Wm^{-2}\ \mu m^{-1}$
E^{+}	Internally generated fluxes	$Wm^{-2}\ \mu m^{-1}$
E_{cs}	Thermal emitted fluxes from individual leaves in the sun	$Wm^{-2}\ \mu m^{-1}$
H_{cd}	Thermal emitted fluxes from individual leaves in the shade	$Wm^{-2}\ \mu m^{-1}$
E_{sun}	Solar irradiance on the horizontal ground surface or at the top of canopy	$Wm^{-2}\ \mu m^{-1}$
f_s	Leaf area projection factor in the direction of the sun	-
$\overline{T}_s$	Average annual temperature	^0C
c_p	Heat capacity	$Jkg^{-1}K^{-1}$
T_s	Temperature of an element	^0C
T_a	Temperature above the canopy	^0C
q_s	Humidity in the stomata or the soil pores	$kg\ m^{-3}$
q_a	Humidity above the canopy	kgm^{-3}
r_a	Aerodynamic resistance	sm^{-1}
r_c	Stomatal or soil surface resistance	sm^{-1}
∇_v	Slope of the saturated vapour pressure temperature relationship	$kPa\ K^{-1}$
R_n	Net radiation flux density above the canopy	$W\ m^{-2}$
G_o	Soil heat flux density	$W\ m^{-2}$
ρ_{air}	Mean air density at constant pressure	$kg\ m^{-3}$
c_{air}	Heat capacity of moist air per unit mass	$J\ kg\text{-}1K^{-1}$
e_{sat}	Saturated vapour pressure	kPa
e_{act}	Actual vapour pressure	kPa
$r_{a,h}$	Aerodynamic resistance for heat transport	sm^{-1}
h_c	Crop height	m
u_z	Wind speed	$m\ s^{-1}$
Z_r	Rooting depth	m
P_i	Depth of precipitation	mm
RO_i	Runoff from the soil surface	mm
CR_i	Capillary rise from the ground water table	mm
ETc_i	Crop evaporation	mm
DP_i	Water loss out of the root zone by deep percolation	mm
Iw	Irrigation water	mm
P_e	Gross precipitation	mm
V_c	Surface water flowing in the irrigated area	mm
ρ	Reflectance from the leaf	-
θl	Leaf inclination angle	radian
φl	Leaf azimuth angle	radian
ω	Frequency of the diurnal cycle	$rad\ s^{-1}$
Γ	Thermal inertia of the soil	$JK^{-1}m^{-2}s^{-1/2}$
ρ_a	Density of air	$kg\ m^{-3}$
λ	Evaporation heat of water	Jkg^{-1}
γ_{air}	Psychometric constant	$kPa\ K^{-1}$
θ_{FC}	Water content at the field capacity	m^3m^{-3}

θ_{wp}	Water content at the wilting point	m^3m^{-3}
t	Transmittance of the leaf	-

LIST OF FIGURES

LIST OF TABLES

LIST OF ACRONYMS

ABL	Atmospheric Boundary Layer
AOI	Area of interest
ASL	Atmospheric Surface Level
BAS	Bulk Atmospheric Similarity
CCA	Culturable Command Area
CDF	Cumulative Distribution Function
CWC	Central Water Commission
DF	Depleted Fraction
DOY	day of the year
DPR	Delivery Performance Ratio
ECMWF	European Centre for Medium Range Weather Forecasts
ET	Evapotranspiration
ETa	Actual Evapotranspiration
ETp	Potential Evapotranspiration
FAO	Food and Agricultural Organization
FAR	Field Application Ratio
FVC	Fractional Vegetation Cover
GDP	Gross Domestic Product
GIS	Geographic Information Science
LAI	Leaf Area Index
LST	Land Surface Temperature
MAE	Mean Absolute Error
MODIS	Moderate Resolution Imaging Spectroradiometer.
NCAP	National Centre for Agricultural Economics and Policy Research.
NDVI	Normalized Difference Vegetation Index
RAW	Readily Available Water
rbs	soil boundary resistance
RE	Relative Evapotranspiration
RMSE	Root Mean Square Error
rss	soil surface resistance
RTMo	Radiative Transfer Model, optical
RTMt	Radiative Transfer Model, thermal
SCOPE	Soil Canopy Observation, Photochemistry and Energy Fluxes
SEBS	Surface Energy Balance System
SVAT	Soil Vegetation Atmosphere Transfer
TAW	Total Water Available

1. INTRODUCTION

Water is gradually becoming a scarce commodity worldwide especially in the developing countries. With the increasing need of providing food and water security for an ever increasing population the availability, usability and affordability of water is becoming a major challenge. Efficient use of this resource is demanded. However this requires innovation and more precision in its utilization, especially where it is used in abundance, like agriculture. In spite of technological advancements in pressurized irrigation techniques, a substantial amount of land worldwide, especially in countries like India (Briscoe & Malik, 2005), is still irrigated by surface irrigation. Here water is transported through canals up to the farmer's field for sustaining crop growth. With agriculture being the most dominant water user it is essential to develop and improve existing technologies for more efficient use of this precious resource especially in countries with huge population like India.

1.1. Irrigation and Water Management

Efficient water demand and supply management provides water and food security to a country. Due to the pressure on water resources in India it is projected that by 2050, seventeen out of twenty major river basins will be water stressed (Gupta & Deshpande, 2004). The total irrigation potential created up to the current Five Year Plan is 41637.86 thousand hectares (CWC, 2011). To manage an irrigated area on such a large scale it is essential to develop cost effective technologies to estimate the precise amount of water needed for utilizing the existing water resource more judiciously. It is predicted that India will to get 10 to 20 percent more intense rainfall but also longer dry spells, due to climate change. Similary evaporation will be also be increasing and thus provide a major pressure on limited water resources is awaited, affecting the ground water balance in many regions in India (NCAP, 2011).
Hence from the irrigation and water management point of view, rainfall-runoff and evaporation remain the most important components of the hydrologic cycle affecting agriculture. While rainfall can be directly measured by gauges, the precise quantification of evaporation form soil and plant still remains a challenge. The need of the hour is to quantify evaporation/evapotranspiration on a temporal and spatial basis and thus the importance of satellite based remote sensing and GIS is realized.

1.2. Evapotranspiration through space

Evapotranspiration (ET) describes water evaporated from both soil and plant. This loss of water from the surface needs to be replaced through irrigation (FAO 56, 1998). More irrigation leads to waterlogging while less results in impacts on agricultural production. Estimates show that in India almost 7×10^6 hectare of the Cultural Command Area (C.C.A) has already been affected by salinity and water logging (Joshi & Tyagi, 1994). Precise quantification of ET in space and time is therefore essential to avoid over irrigation or under irrigation of irrigated lands. This in turn saves water and enhances crop yield.
The potential of remote sensing techniques and water resource management has already been proven to be immense. However, ET cannot be directly measured from space. Hence representative measurements of ET relevant physical parameters need to be observed, (Su, 2002; Su et al., 2003; W. J. Timmermans et al., 2007; Wang et al., 2011; Xiong et al., 2006; Yang et al., 2004). From these land surface parameters ET can then be calculated, using One-Source and Two-Source Surface Energy Balance Models(Kalma et al.,

2008) such as SEBS and SEBAL. As evapotranspiration is highly dependent on the land surface temperature, these models demand the presence of thermal bands in the satellite sensor. In many studies SEBS is used to estimate ET (Su, 2001, 2002, 2005; Su et al., 2003). SEBS is recommended over other surface energy balance algorithms because it is a physical based model.

At the same time the major challenge before the scientific community, is how to improve the accuracy of the information extracted from free of charge low resolution imagery. Hence improvements in irrigation management using ETa calls for integrating agro-metrological data along with satellite data and GIS tools through existing models like Surface Energy Balance Systems (SEBS), (Su, 2002) and SVAT models as Soil Canopy Observation, Photochemistry and energy fluxes (SCOPE),(C. van der Tol et al., 2009) and evaluating their performances, based on certain indices. The output of scope can aslo be used as a validation data(C. van der Tol et al., 2009).

1.3. Irrigation Performance Assessment

The most critical element for improvement in an irrigated area is to assess its performance (M. G. Bos et al., 2005; M. G. Bos, Kselik, R.A.L., Allen, R.G., Molden, D., 2008; Cuevas et al., 2010; de Fraiture et al., 2010; Knox et al., 2012; Reeling et al., 2012) . An ideal or reference irrigation is the one that provides the required water at the right time and right amount for the entire area with minimum losses (Zerihun et al., 1997). Water balance indicators such as, Delivery Performance ratio (DPR), Depleted Fraction(DF), Relative evapotranspiration (RE), Crop water deficit (CED) and Field Application ratio (FAR) are mostly used for this(M. G. Bos, 1997). These indicators can assess the irrigated areas in time and space. Several researchers have reported the successful use of remote sensing based tools for assessing irrigation performance,(Ahmad et al., 2004; W. G. M. Bastiaanssen et al., 1998; M. G. Bos et al., 2005; Raju et al., 2008; Ray et al., 2002). They have also reported that remotely sensed estimates of crop ETa directly represents the crop growth conditions and is a better estimate of ETa, when compared to field measurements. They recommend that when this method is used as an input for any spatial irrigation scheduling program, it minimizes the impact of over and under irrigation (Ray & Dadhwal, 2001). Further the integration of various space bound platforms for more precise information on estimation of ETa is encouraged (Anderson et al., 2012) and is necessary in view of the actual image limitations.

1.4. Justification

The contribution of agriculture to the Gross Domestic Product (GDP) is gradually diminishing in India. Huge investments in irrigation infrastructure ensure the success of food security programs. This increases the living standards of the local population, contributing to the overall increase in GDP of a country (Briscoe & Malik, 2005; CWC, 2011). Hence it is essential to regularly evaluate the performance of these irrigation projects.

Irrigation water supply and management in India is based on government estimates and not on the level of the farmer's demands. Presently these evaluations are only based on utilization of resources such as production and profitability. However a proper alternative should be on the use of spatial and temporal operational indicators that not only refer to production and profit, but also to the quality of service, crop water demand, crop water use and drainage. This is also due to the fact that manual, spatial and temporal assessment is quite time consuming and expensive, which water boards cannot afford.

The issue of how adequately and equally irrigated water is distributed on a temporal and spatial scale (water equity) is not evaluated on a plot scale. Today, this is one of the major problems being faced at any canal irrigated area in India, only point based measurements are used to assess water needs for an irrigated area, because, the time and budget constraints . This leads to an uneven distribution of water because point based measurements cannot give precise output for irrigated areas that are spread over large areal extents. Spatial and temporal data is better in accessing performances when compared with point based in situ measurements (Zwart & Leclert, 2010).

1.5. Problem Statement

With the advancements in image processing and increase in computational power, the use of remote sensing and merging of satellite data to extract spatial and temporal information for precision agriculture is growing (Anderson et al., 2012).The question of accuracy for the desired output still remains (Ha et al., 2012a) especially in case the agricultural plots being small. The average agricultural plot size in India is 1.4 ha(Thapa & Gaiha, 2011). The frequency distribution of plot size at the Samarakalwana village, a part of the CCA is shown in Figure 1-1.Small plots are difficult to manage, but do exist in almost all CCA's in India. Individual farmers generally grow crops to fulfil their needs; hence a large heterogeneity in a CCA exists. This breeds in uncertainties if ETa is measured at low resolutions. However high resolution images are not free and have a low revisit frequency. While low resolution satellites have a high revisit frequency.

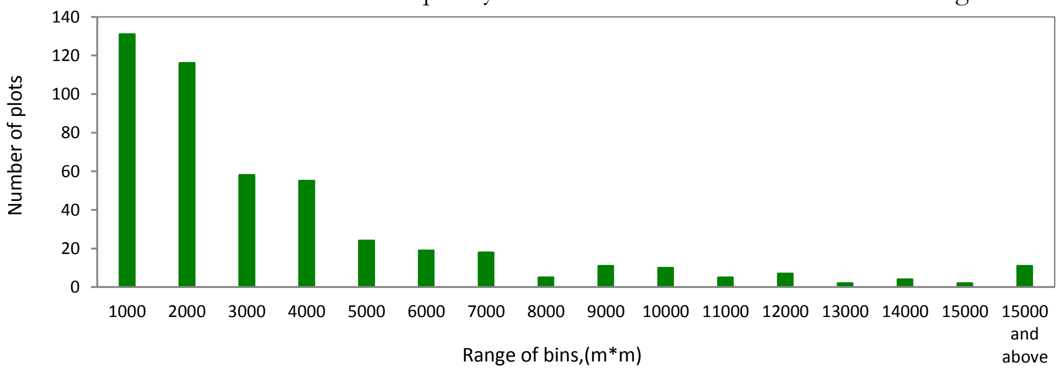

Figure 1-1 The frequency distribution of agricultural plot at the Samrakalwana village.

1.6. Research Objectives and Questions

The aim of this research is to upscale low resolution ETa and asses an irrigated area based upon water balance indicators. Open source remotely sensed images are used to quantify ETa. Low resolution images generally require complementation to generate information on an irrigation plot scale.

This research develops an affordable methodology to reduce uncertainties by enhancing resolution while extracting information from a low resolutions image through an upscaling of low resolution information. Considering this and the above mentioned challenges, a study entitled "Irrigation Performance Assessment of an Irrigated Area using SEBS and SCOPE." has been undertaken to find solutions to the research problems through achieving the following specific objectives:

1.6.1 Specific Objectives

The problems discussed in paragraph 1.5 and the objectives of this research shall be achieved through reaching to the specific objectives given below:

1. Upscaling ETa map.
    a. Quantification of ETa using SEBS with MODIS low resolution (1km) images.
    b. Upscaling of SEBS-MODIS generated ETa maps using land use/land cover map.
2. Validation of upscaled ETa with SCOPE generated ETa.

a. Estimation of ETa at plot scale using SCOPE with the assistance of in-situ measurements.

3. Assessment of irrigated area experiencing performance gaps, based upon ETa estimates.

1.6.2 Research Questions

Taking into consideration the above mentioned facts, an attempt is being made to answer the following research questions. The research questions are as follows:

1. Does the upscaling of SEBS increase comparisons with measurements or simulations of actual evapotranspiration?
2. How can the performance of an irrigated area be accessed by performance indicators based on ETa?
3. What is the temporal variation of water stress in the irrigated area?
4. What should be the measures to reduce the uncertainties when measuring performance?
5. Does this experience produce practical recommendations to improve the performance of the irrigate area? What are they?

1.6.3 Hypothesis

Seepage and conveyance losses in the irrigated area are not considered in the study. They are related to the distribution method and the present state of maintenance. Also this assumption was made because no high resolution soil moisture data was available. The spatial distribution of the water stress coefficient is assumed to be uniform over the entire pixel.

1.7. Significance of the Study

The study is intended to quantify the actual evapotranspiration for the irrigated area. Due to climate change phenomena India is experiencing more rainfall and long dry spells resulting more loss of water in the form of evapotranspiration in the process, depleting the much needed water resource (CWC, 2011). An effort is made to precisely quantify, the amount of water lost due to this phenomenon using MODIS images, and in-situ meteorological observations on a temporal and spatial basis. It gives an insight as to how SEBS generated low resolution ETa is upscaled. The SCOPE generated ETa for wheat grown in the irrigated area is used to validate the high resolution SEBS ETa, helping in reducing uncertainties and increasing precision for low resolution images (Ha et al., 2012b; Hwang et al., 2011; Kim & Barros, 2002; J. Timmermans et al., 2011) . This will lead us to quantify the actual amount of irrigation water needed for the irrigated area. This will help the researchers, policy makers, government officials and water user associations to identify potential gap and recommend measures to use the scarce water resource more judiciously.

2. THEORY

This chapter deals with the theoretical considerations involved in the estimation of actual evapotranspiration at a local/regional scale as well as farmer's field or plot scale.
The processes are explained as follows:

1) The estimation of atmospheric turbulent fluxes over an irrigated area.
2) Estimation of ETa by considering land surface parameters on the basis of energy balance estimates at dry and wet conditions (Su, 2002).
3) The integration of a detailed process model which integrates radiative transfer and energy balance approach through a combination of a cascade of models integration soil-canopy spectral radiances, photosynthesis, fluorescence, temperature and energy balance at the level of individual leaves as well as he canopy (C. van der Tol et al., 2009).
4) Potential and reference evapotranspiration (FAO 56, 1998) over an irrigated cropped area.
5) Evaluate the performance of an irrigated area, based upon water balance indicators(M. G. Bos, 1997).

Irrigation refers to the artificial application of water to crops. It compensates the loss of water from the cropped fields released in the form of crop evapotranspiration and equals the crop water requirements. This amount is also referred as irrigation water requirement or complementary irrigation and represents the difference between the crop water requirement and effective precipitation. The irrigation should also include an extra to account for the seepage losses, salinization processes and water compensated for the non-uniformity of water application which is insignificant in the case of efficient design of agricultural fields. Quantification of irrigation water requires understanding the processes that leads to the release of water from the irrigated cropped areas in the form of water vapour. These processes include the conversion and release of liquid water to water vapour from soil in the form of evaporation and it's vaporization from crops as transpiration. Since these processes are occurring simultaneously in an unified approach as the one selected in this research, they are quantified together and are referred as evapotranspiration (ET). The net radiation balance and the availability of soil moisture are leading the partition between evaporation and heat, among other spatial variables. In order to precisely quantify the irrigation amount for any irrigated area it is very essential to understand the above mentioned processes.

2.1. Evapotranspiration

Evapotranspiration represents the return of precipitated water stored in the soil to the atmosphere (Thornthwaite & Mather, 1951). It results due to the difference between water vapour pressure from the evaporating surface and that of the surrounding atmosphere. The exchange of the saturated air surrounding the evapotranspiration object by drier air greatly depends upon the wind speed, solar radiation, air temperature, air humidity over the object of consideration (Cammalleri et al., 2012; Shenbin, 2006). Quantification of evapotranspiration is essential to manage irrigated areas more efficiently. Several methods are available to measure ET, but in recent years remote sensing based approaches have shown promising results (Cammalleri et al., 2012). Here an approach is made into estimating ETa at plot and regional scales. At regional scale ETa is generated by SEBS (Su, 2002) and at plot scale using SCOPE (C. van der Tol et al., 2009) .and SEBS (Su, 2002) does it at the scale of pixel size from available imagery.

2.1.1. Evapotranspiration at the regional scale

SEBS, developed by (Su, 2002) is a 1-D vertical remote sensing algorithm for the estimation of the atmospheric turbulent heat fluxes or evapotranspiration when the latent heat flux is expressed in terms of water depth, using satellite earth observation data. It can generate instantaneous maps that can be integrated to daily, monthly and annual evapotranspiration in a semi-arid environment using complementary algorithms (Su et al., 2003). It uses the Bulk Atmospheric Similarity (BAS) and Monin-Obukhov atmospheric surface layer (ASL) similarity for the estimation of turbulent fluxes. SEBS accounts for surface heterogeneity in the estimation of roughness height for heat transfer. The uncertainties in derived latent heat flux and evaporative fraction is limited since SEBS considers energy balance at the limiting cases (dry and wet limits). The three sets of tools the model consists of are to derive the land surface parameters from the satellite data, to determine the roughness length of heat transfer and to determine the evaporative fraction considering the limiting cases for energy balance (Su, 2005).
The three most basic inputs required by SEBS are shown in Figure 2-1 and are given below:

1) Land surface parameters obtained through remote sensing (albedo, land surface temperature, emissivity, leaf area index, vegetation fraction, vegetation height).
2) Meteorological data such as air temperature, air pressure, humidity, wind speed at reference height.
3) Downward short wave solar radiation and downward longwave radiation.

The detailed processes involved in SEBS are explained in Appendix.

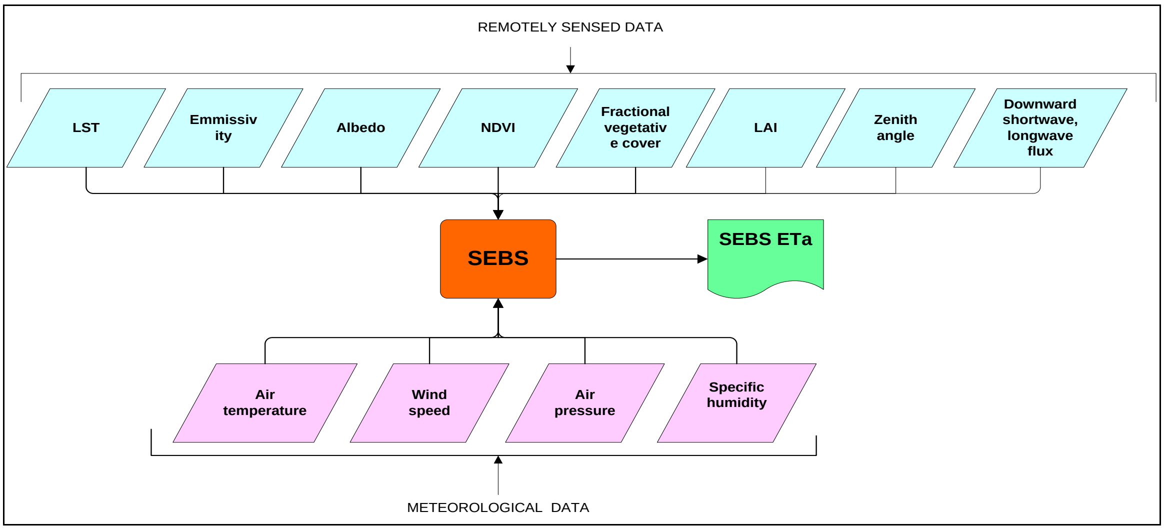

Figure 2-1 Remotely sensed, Processed Level 2 MODIS and meteorological data used in SEBS

2.1.2. Up scaling of low resolution actaul evapotranspiration.

The low resolution ETa obtained through SEBS for an irrigated area represents the total evaporation from different land cover types, inside individual pixel. This low resolution SEBS ETa, is disaggregated to obtain up scaled or high resolution ETa, for each of the different land cover type contributing to the low resolution ETa and is explained by the following equations:

$$K_s = \frac{AET_{(lr,SEBS)}}{ET_p} \qquad 2.1$$

Where,

Ks is the transpiration reduction factor depending on available soil water, (similar to FAO approach), $AET_{(lr,SEBS)}$, is the low resolution, actual evapotranspiration obtained through SEBS

ET_p is the potential evapotranspiration.

The high resolution disaggregated actual evapotranspiration is expressed as:

$$AET_{(hr,SEBS)} = AET_{(lr,SEBS)} * W_{(hr)} \quad 2.2$$

Where,

$AET_{(hr,SEBS)}$, is the disaggregated upscaled

$AET_{(lr,SEBS)}$, $W_{(hr)}$ is the weighted high resolution of an individual land cover class.

This is expressed as:

$$W_{(hr)} = \frac{K_{c,hr}}{\sum K_{c.hr}} \quad 2.3$$

Where,

Kc is the crop coefficient depending upon the plant growth stages.

2.2. Evapotranspiration at the plot scale

An integrated model of soil-canopy radiances, photosynthesis, florescence, temperature and energy balance SCOPE, (C. van der Tol et al., 2009), is a vertical (1-D) integrated relative transfer and energy balance model, linking the visible and thermal infrared radiance spectra (0.4 to 50μm) as observed above the canopy, to the fluxes of water, heat and carbon dioxide as a function of vegetation structure and the vertical profiles of temperature. The output is the turbulent heat fluxes along with the spectrum of outgoing radiation in the viewing direction for a single leaf as well as the canopy level. SCOPE is used on a plot scale to retrieve evapotranspiration from the ground observations and meteorological data. The relevant theory of the model used in this study is explained below.

2.2.1 Model structure

The model structure comprises of a structured cascade of separate modules which can be used as standalone or as integrated as shown in Figure2-2. They are connected by exchanging their inputs and outputs. The modules are executed in the following manner.

1. Firstly, a semi analytical optical Radiative Transfer Module (Jacquemoud et al., 2009; Verhoef & Bach, 2007) calculates the top of canopy outgoing bidirectional optical radiation.
2. Afterwards another radiative transfer module simulates the multiple scattering and emission of thermal radiation. It enables the top of canopy thermal radiances observed under multiple viewing angles to be related to the temperatures of sunlit and shaded soil and leaves (W. Verhoef et al., 2007).
3. This is followed by the third, an energy balance module that distributes the net radiation over turbulent air fluxes and heat storage.
4. Finally, a radiative transfer module to calculate the top of canopy radiance spectrum of fluorescence form leaf level chlorophyll fluorescence and the geometry of the canopy.

Iteration is carried out between the thermal radiative transfer module(2) and the energy balance module (3)to match the input of the radiative transfer model with the output of the energy balance model and also the input of the energy balance model with the output of the radiative transfer model. The distribution of irradiance and net radiation over surface elements such as leaves and soil, obtained as an output of the radiative transfer module, serves as an input for the energy balance module and hence the turbulent energy fluxes are obtained. The energy balance components of the model output is used in this study and discuss it in detail in the following section.

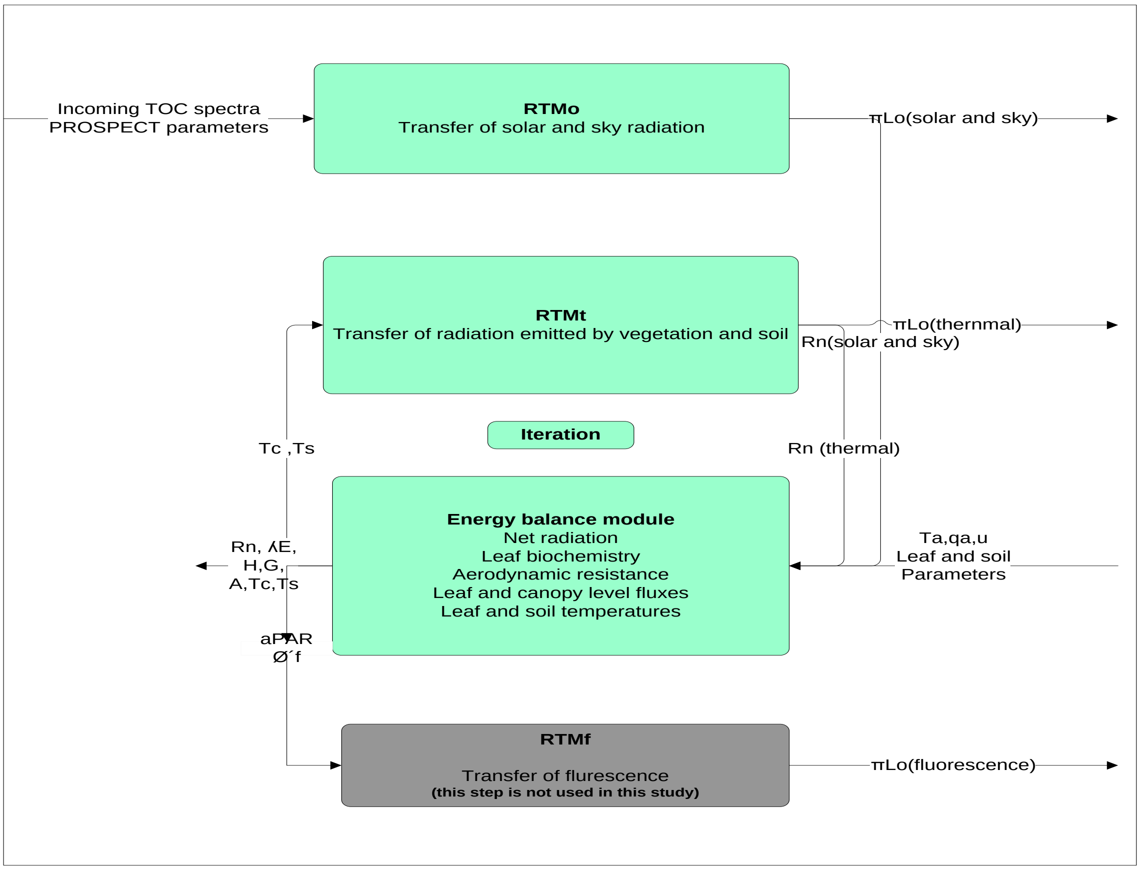

Figure 2-2 Schematic overview of SCOPE model structure

2.2.2 The Energy Balance

The model calculates the energy balance for each element and distributes the net radiation over turbulent air fluxes and heat storage. An element in the model is best described by the geometry of the canopy which is assumed to be homogeneous and in one dimensional. Hence the variation of macroscopic properties in the horizontal plane along with the clumping of twigs and branches are neglected. The leaves and soil are divided into classes which receive a similar irradiance. These classes are called elements. The energy balance equation for each element is the same as given in equation 2.4.

$$R_n = G_0 + H + \lambda E \qquad 2.4$$

Where,

R_n is the net radiation [Wm^{-2}]
G_0 is the ground heat flux [Wm^{-2}]
λE is the latent heat flux [Wm^{-2}]
H is the sensible heat flux. [Wm^{-2}].

The net radiation of a layer is the weighted sum of the contributions from shaded and sunlit leaves with different leaf angles, while the net radiation of the canopy is the sum of contributions of radiation of individual layer. The net spectral radiation on a leaf is the difference of the absorption and the total emission from it's both the sides. The equations for shaded and sunlit leaves are given below:

$$R_n (x) = [E^-(x) + E^+ (x) - 2H_{cd} (x)](1 - \rho - \tau) \quad 2.5$$

$$R_n(x, \theta_l, \varphi_l) = \{|f_s|E_{sun}[+E^-(x) + E^+(x)] - [2H_{cs}(x, \theta l, \varphi l)]\}(1 - \rho - \tau) \quad 2.6$$

Where, ρ and τ are reflectance and transmittance of the leaf. E^- and E^+ are the sum of externally and internally generated fluxes [Wm^{-2} μm^{-1}] while E_{cs} and H_{cd} are the thermal emitted fluxes from individual leaves in the sun and in the shade [Wm^{-2} μm^{-1}]. The solar irradiance on the horizontal ground surface or at the top of canopy is E_{sun} [Wm^{-2} μm^{-1}]. while , $\theta l[rad]$, is the leaf inclination angle, $\varphi l, rad,$ is the leaf azimuth angle and f_s, is the leaf area projection factor in the direction of the sun[-] .

The model only considers the heat storage G, for the soil, while neglecting the heat storing capacity of the leaves. It is calculated with a discreet version of the force restored method (Bhumralkar, 1974), while the other fluxes are calculated from the vertical gradients of temperature and humidity for soil and foliage in accordance with the Ohm's law for electrical current:

$$G = \frac{\Gamma}{\sqrt{2\omega\Delta t}}(|T_s(t + \nabla t) - T_s| + \omega\nabla t[T_s(t) - \overline{T_s}]) \quad 2.7$$

$$H = \rho_a c_p \frac{T_s - T_a}{r_{ak}} \quad 2.8$$

$$\lambda E = \lambda \frac{q_s(T_s) - q_a}{r_{ak} + r_{ck}} \quad 2.9$$

Where,

ω is the frequency of the diurnal cycle [rad s^{-1}]

Γ is the thermal inertia of the soil in [$JK^{-1}m^{-2}s^{-1/2}$]

$\overline{T_s}$is the average annual temperature[^{0}C]

ρ_a is the density of air [kg m^{-3}],

c_p is the heat capacity [$Jkg^{-1}K^{-1}$]

λ is the evaporation heat of water [Jkg^{-1}]

T_s is the temperature of an element [^{0}C]

T_a is the air temperature above the canopy [^{0}C]

q_s is the humidity in the stomata or the soil pores [kg m^{-3}]

q_a is the humidity above the canopy [kgm^{-3}]

r_a and r_c are the aerodynamic resistance and stomatal or soil surface resistance [sm^{-1}]

Both H and λE are calculated for each surface element separately while equation 2.9 holds for leaves which only have one side contributing to transpiration. If both the sides contribute to transpiration then $r_{ck}$is half the one sided value for r_{ck}.

2.3. Reference Evapotranspiration from Penman-Monteith

The estimation of the Potential Evapotranspiration ETpot [mm day^{-1}] will be obtained using the Penman-Monteith equation (Allen et al., 1998.; Monteith, 1965; Rijtema, 1965; Smith, 1992) as given by equation 2.7.

$$ETp = \frac{86400 * 10^3}{\lambda \rho w} \frac{\nabla v(Rn - Go) + \rho_{air}\left[\frac{esat - eact}{ra,h}\right].C_{air}}{\Delta v + \gamma air\left[1 + \frac{rc,min}{ra,h}\right]} \quad 2.10$$

Where,

∇_v is the slope of the saturated vapour pressure temperature relationship [kPa K^{-1}]
R_n is the net radiation flux density above the canopy [W m^{-2}]
G_o is the soil heat flux density [W m^{-2}]
ρ_{air} is the mean air density at constant pressure[kg m^{-3}]
c_{air} is the heat capacity of moist air per unit mass [J kg-1K^{-1}]
e_{sat} is the saturated vapour pressure [kPa],
e_{act} is the actual vapour pressure [kPa]
λ is the latent heat of vaporization [J kg^{-1}]
γ_{air} is the psychometric constant [kPa K^{-1}]
r_c is the minimum value of the surface resistance of canopy when water is not limited. In this condition the canopy resistance r_c reaches a maximum value $r_{c,min}$ [sm^{-1}]
$r_{a,h}$ is the aerodynamic resistance for heat transport [sm^{-1}]. The aerodynamic resistance $r_{a,h}$ [sm^{-1}] will be calculated as a function of crop height h_c,[m] and wind speed u_z [m s^{-1}],(Howell & Evett, 2011).

2.4. Irrigation depth

Water is applied to an irrigated area when the rainfall is insufficient and to compensate for its loss due to evapotranspiration. The most important objective of applying water to an area is to supplement this loss at the right period with the right amount. The soil water balance of the root zone is obtained on a daily basis, hence planning the exact amount of water needed to irrigate. The soil water availability in the root zone and root zone depletion at the end of each day is calculated. The total water in the root zone is expressed as:

$$TAW = 1000(\theta_{FC} - \theta_{WP})Z_r \tag{2.11}$$

Where,

TAW, is the total available water in the root zone [mm],
θ_{FC} is the water content at the field capacity [m^3m^{-3}],
θ_{wp} is the water content at the wilting point [m^3m^{-3}]
Z_r is the rooting depth[m].

The fraction of the TAW that the crop can use or extract from the root zone without experiencing water stress is the readily available water. This is a fraction of the TAW and is expressed as:

$$RAW = pTAW \tag{2.12}$$

Where,

RAW, is the readily available water in the root zone [mm],
p is the average fraction of the total available soil water that can be depleted from the root zone before moisture stress occurs (FAO 56, 1998).

The root zone depletion, D_r in mm is expresses as:

$$D_r = TAW\big(1 - K_s(1-p)\big) \tag{2.13}$$

The initial depletion $D_{r,i-1}$ in mm is expressed as :

$$D_{r.i-1} = 1000(\theta_{FC} - \theta_{i-1})Z_r \tag{2.14}$$

Where, θ_{i-1} is the average soil water content for the effective root zone [m^3m^{-3}]. The net irrigation depth I_i in mm, on a daily basis that infiltrates the soil and to be compensated by irrigation is expressed as:

$$I_i = D_{r,i-1} - D_{r,i} - (P - RO)_i - CR_i - ET_{c,i} + DP_i \tag{2.15}$$

Where,

P_i is the depth of precipitation[mm],

RO_i, is the runoff from the soil surface[mm],

CR_i is the capillary rise from the ground water table [mm],

$ETc_{i\ id}$ is the crop evaporation[mm day^{-1}]

DP_i is the water loss out of the root zone by deep percolation.

The ETc is going to be extracted from high resolution ETa.

2.5. Performance assesment

Performance assessment of an irrigated area supports the planning and its irrigation implementation (M. G. Bos, 1997; M.G. BOS et al., 1991). The ETa based criteria for assessment of an irrigated area is to ensure equity in the supply of water and to optimize the efficiency of water distribution. The ETa based performance indicators are as following:

1. Delivery performance ratio: The DPR is defined as the actual water delivered as intended for the crop growing period and at any location in the irrigated area (Clemmens & Bos, 1990).
2. Depleted fraction: The DF compares the actual evapotranspiration of the irrigated area to the total precipitation received plus the surface water applied through irrigation.
3. Relative evapotranspiration: The RE explains the adequacy of the irrigation water delivered to the irrigated area as a function of time.
4. Crop water deficit: The CWD is defined as the difference between the potential and actual evapotranspiration of the cropping pattern within an area over a period of time.

$$DPR = \frac{Iw(actual)}{Iw(intended)} \tag{2.16}$$

$$DF = \frac{ET_a}{P_e + V_c} \tag{2.17}$$

$$RE = \frac{ET_a}{ET_p} \tag{2.18}$$

$$CWD = ET_p - ET_a \tag{2.19}$$

Where,

Iw, is the irrigation water[mm]

P_e is the gross precipitation received in the irrigated area[mm]

V_c is the surface water flowing in the irrigated area[mm]

3. STUDY AREA

The study area, a part of the Tons river basin falls approximately between Latitude of 25°16' 31"N and Longitude of 82°4'55"E. The origin of the canal is at 25°2'34.44"N and 81°45'27.3"E. The soils at the irrigate area are clay loam to sandy loam (230 km^2) and the remaining of soils are loam to sandy loam (71.4km^2). The major crops grown are wheat followed by pulses and potato. Orchard consisting of citrus plants are also grown in the CCA. The total C.C.A is 301.4km^2 and has achieved its full potential.

The study area falls in the southern part of the Allahabad, the most populous district of Uttar Pradesh. It is subjected to a humid subtropical climate and has an annual mean temperature of 26 ^{0}C with a minimum temperature of 2 ^{0}C in winters and a maximum of 48 ^{0}C in summers. The hot and dry summers begins from the month of March and carries on till June with May being the hottest. While winters falls between the months of November till end of February.

The main source of irrigation for the irrigated area is the Tons River also called the Tanus River. Tons River is a tributary of the Ganges River and flows through Madhya Pradesh and U.P. the river originates from the Kaimur Range at an elevation of 610 metres and meets the Ganges after crossing a length of 264 Km at Sirsa near Allahabad. The total drainage area of the river is 16860 km^2.

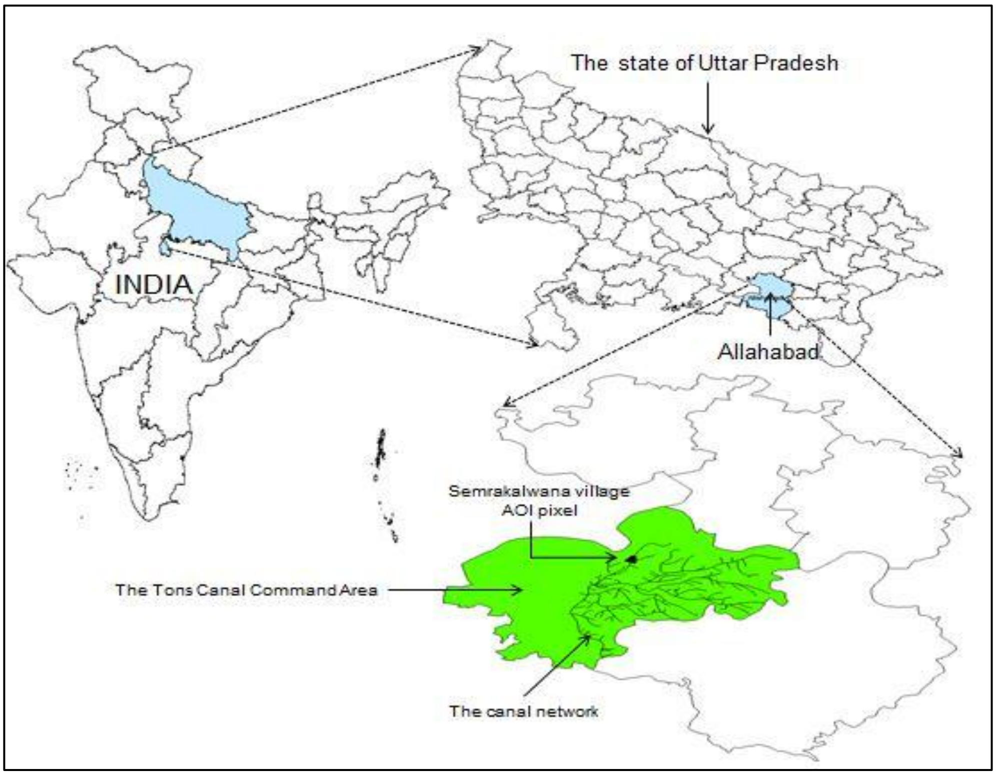

Figure 3-1 The study area "The Tons canal command" in relation to its orientation in U.P. State and India.

3.1. Climate

According to the Weather Report and Forecast of the Indian Meterological Department, 2012 the average minimum and maximum temperature, rainfall, humidity, average rainy days and mean monthly sunshine hours taking into consideration the climate from 1971 to 2000 are shown. The average minimum and maximum monthly temperatures are shown in Figure 3-2.

Allahabad experiences three seasons that are the hot dry summers, extending form mid of March to end of June. This is followed by warm and humid monsoons which begin in early July and lasts till September, as seen in Figures 3.3 and 3.5. The winters are cool and dry and extend from mid of November till the end of February as seen in Figures 3.2 and 3.4. The average monthly rainy days per month and the average monthly sunshine hours are shown in Figures 3-6 and 3-6.

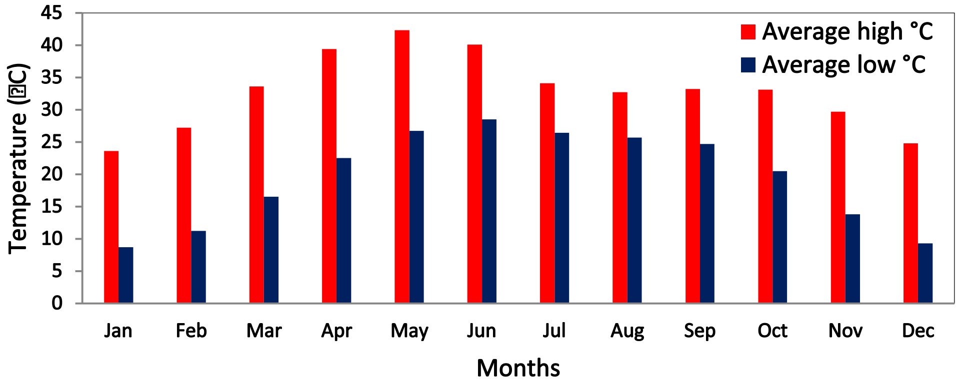

Figure 3-2 Average minimum and maximum temperature at Allahabad.

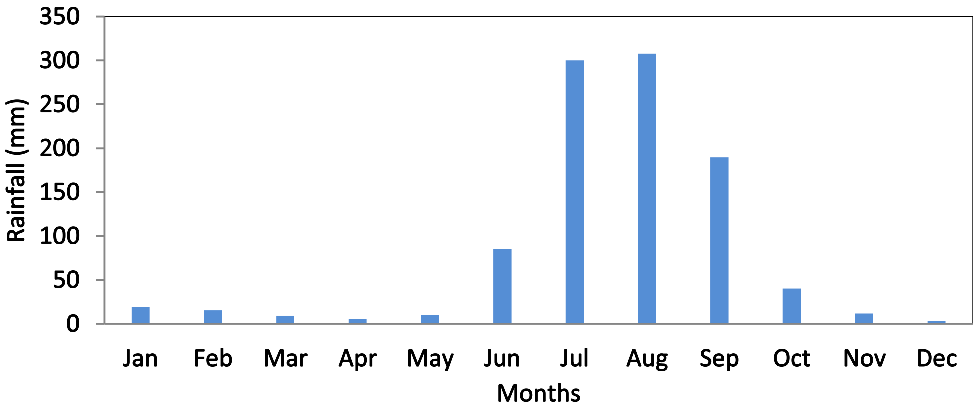

.

Figure 3-3 Average monthly rainfall at Allahabad.

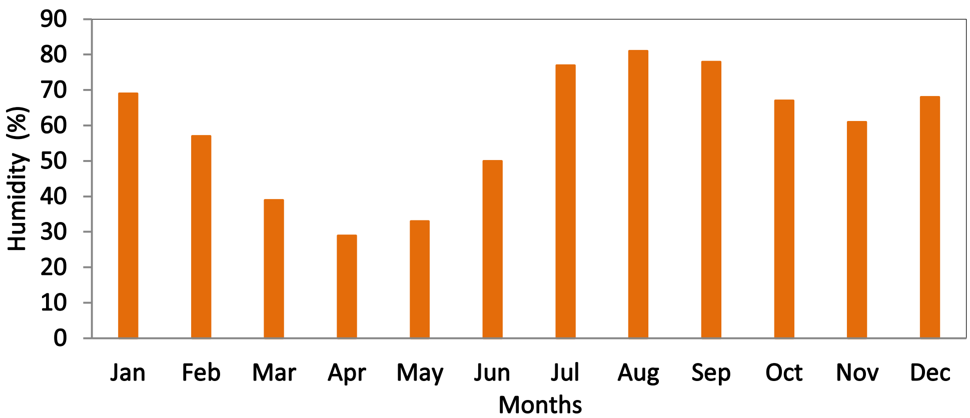

Figure 3-4 Average humidity at Allahabad

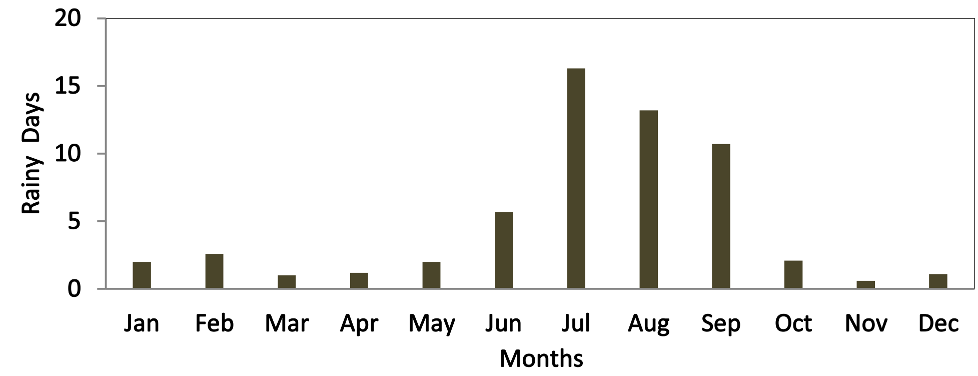

Figure 3-5 Average rainy days at Allahabad.

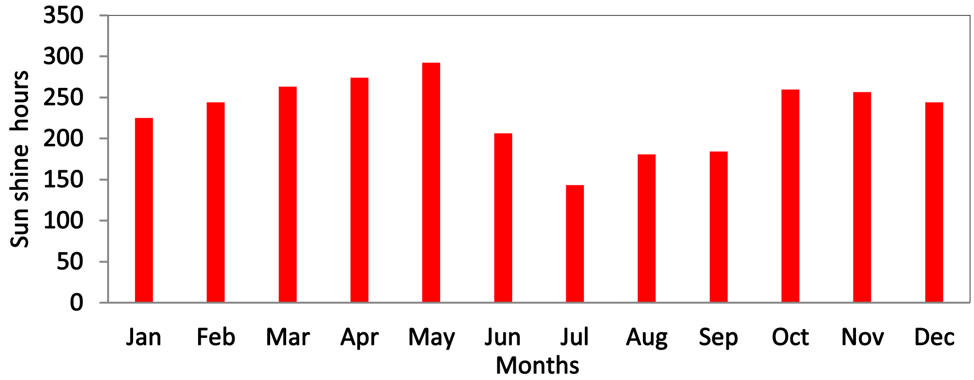

Figure 3-6 Average sun shine hours at Allahabad.

4. METHODOLOGY AND DATA AVALABLE

This chapter deals with the methodology to find solutions for the research problems and objectives discussed in paragraph 1.6.It explains the methodology used to generate ETa at a local scale using SEBS, and as explained in paragraph 2.6. Parallel to it, high resolution ETa, on plot scale is simulated, using SCOPE given in paragraph 2.2. Further GIS tools are used to subset the irrigated area on a pixel basis followed by classification, taking into consideration the land cover classes. This is followed by disaggregation and upscaling the low resolution ETa for each class. Thereafter ETa based performance indicators are obtained to understand the performance of the irrigated areas. The general methodology adopted to upscale a low resolution image and assess the performance of an irrigated area is shown in Figure4-1.The high resolution ETa for the wheat is obtained using SCOPE. The low resolution ETa for the irrigate area is obtained using SEBS. Upscaling of low resolution ETa and generation of high resolution ETa map is done. The upscaled ETa is validated with SCOPE generated ETa. The upscaled ETa is used to quantify the water requirements of the irrigated area. This calculated water requirement is compared with the delivered water and the irrigated area is assessed.

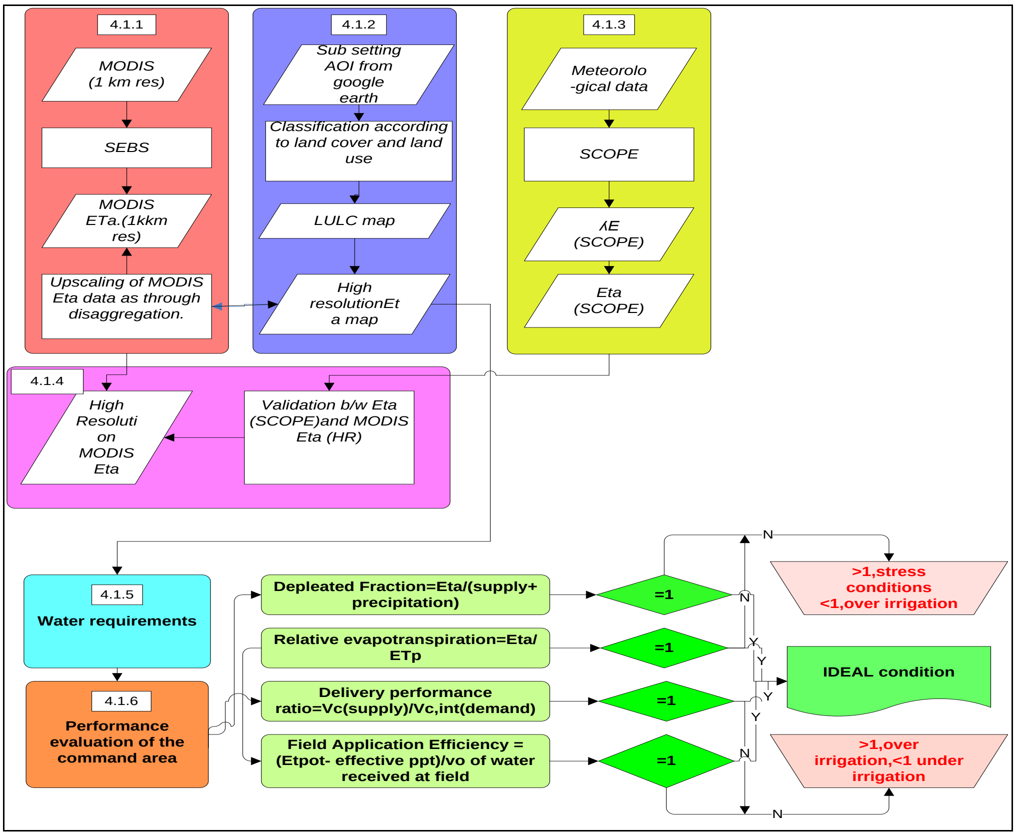

Figure 4-1 Methodology to assess an irrigated area through upscaled SEBS generated ETa.

4.1.1. Determination of ETa at local scale using SEBS.

The Surface Energy Balance System (SEBS) algorithms (Su, 2002), estimates the ETa using MODIS level 2 remotely sensed images downloaded from the USGS site (http://earthexplorer.usgs.gov). SEBS is suitable for ETa estimations on instantaneous basis. Daily estimates are based on the assumption of a constant evaporative fraction for an semi-arid environment (Su, 2002). It is based upon the Bulk atmospheric similarity (BAS) and Monin-Obukhov atmospheric surface layer similarity theories. One of the important features of SEBS is that it considers the surface roughness height for heat transfer and considers energy balance at the limiting case, hence the uncertainties are limited (Su et al., 2003). The input as the land surface parameters considers are given in Table 4-1.

Table 4-1 Input for SEBS.

Albedo	-
land surface temperature	K
Surface emissivity	W m^{-2} K^{-4}
Leaf area index	m^2m^{-2}
Vegetation fraction	-
Vegetation height	m
Air Temperature at reference height	K
Specific Humidity	kg kg^{-1}
Wind speed	m s^{-1}
Reference height	m
Surface solar radiation downwards	W m^{-2}
Surface net solar radiation clear sky	W m^{-2}
Surface thermal radiation downwards	W m^{-2}
Daily sun shine hours	hr
Boundary layer height	m
NDVI	-
Dew point	K
Surface Pressure	kpa

4.1.2. Upscaling of low resolution MODIS ETa

The MODIS derived ETa has a low spatial resolution of 1km. Each ETa pixel contains in itself the average evapotranspiration occurring in an area of 1 km^2. The total evapotranspiration of a pixel is the contribution of all the land cover classes contained in that pixel. In order to obtain the ETa of each class, the MODIS derived low resolution is disaggregated using equation 2.2 and 2.3. Google Earth images were used as the base map for getting the land cover classes. The area corresponding to the area of interest (AOI) pixel was subsetted as shown in as shown in Figure 4-2. Further using GIS tools, classification was done and a raster map based on land use classes was obtained as shown in Figure 4-3. As these classes are allotted values, the desired high temporal and spatial resolution raster maps for the AOI pixel are obtained. Figure 4-4 shows the over lay of the canal over the AOI pixel along with the village map. The raster image of the pixel of interest is shown in Figure 4-5.

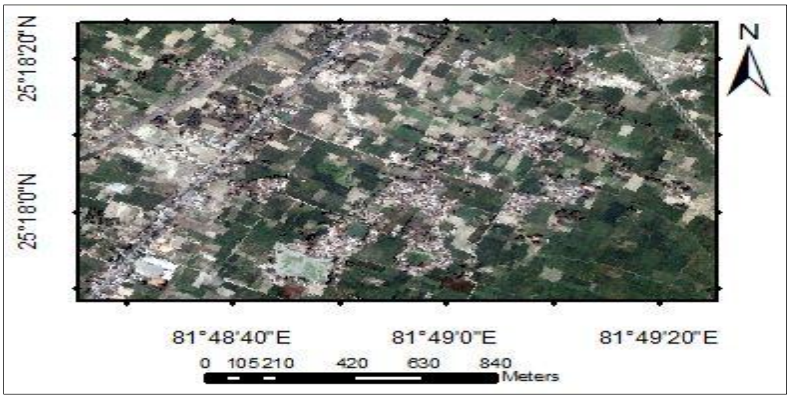

Figure 4-2 Sub setting of the AOI pixel from Google Earth.

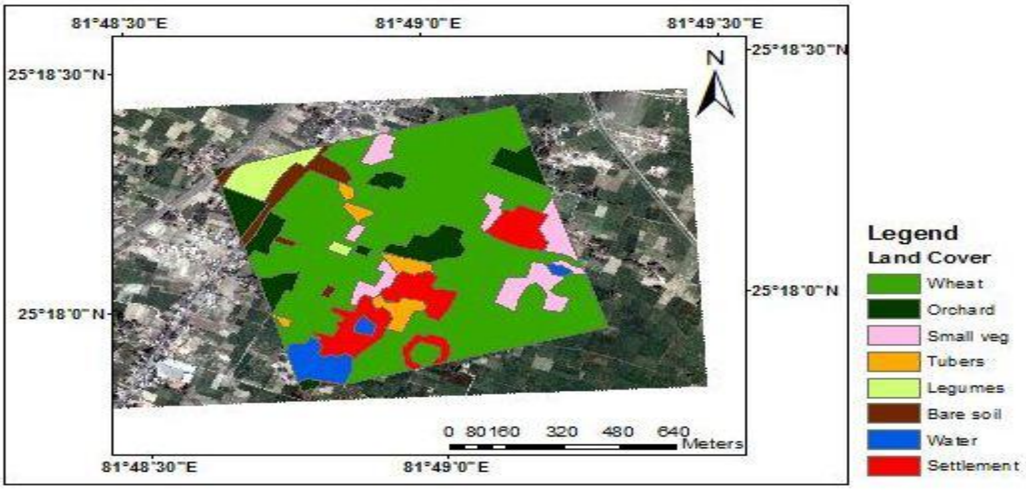

Figure 4-3 AOI pixel classified according to the land cover

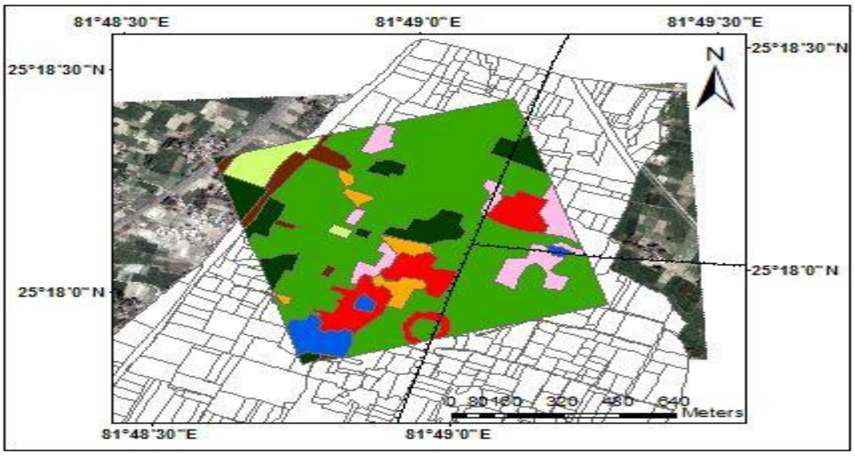

Figure 4-4 Overlay of the village plot map along with the classified map showing the canal passing through the irrigated AOI pixel.

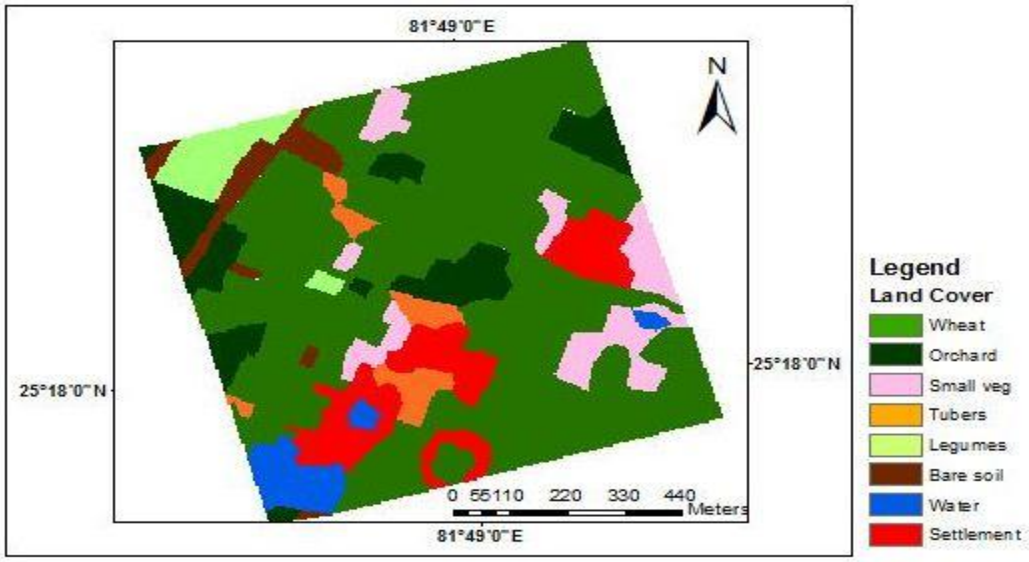

Figure 4-5 Raster map of the AOI pixel showing land cover classes.

4.1.3. Determination of ETa at plot scale using SCOPE.

SCOPE calculates the spectral radiation regime and the energy balance of a vegetative surface at a single leaf as well as canopy level. This makes it one of the most suitable models to calculate the ETa at a high resolution(J. Timmermans et al., 2011; C. van der Tol et al., 2009; W Verhoef et al., 2007). The inputs for SCOPE are given in Table 4-2.

Table 4-2 Input for SCOPE

Solar angle	Degrees
Incoming shortwave radiation	Wm^{-2}
Incoming longwave radiation	Wm^{-2}
Air pressure	hPa
Atmospheric vapour pressure	hPa
Air temperature	^{o}C
Wind speed	ms^{-1}
One sided leaf area index	-
Vegetation height	m
Roughness length of momentum	m
Zero plane displacement	m

Since the Automatic Weather Station did not have sensors to measure the incoming shortwave and longwave radiation, this was downloaded from the ECMWF[1]. The temporal resolution of the data was of three hours. The model was run to obtain ETa for wheat crop grown in Semrakalwana village of Allahabad district for both the winter crop growing seasons of 2010-11 and 2011-12. The orientation of this village on the map of India is shown in Figure 1-1.

The air temperature for both the crop growing seasons was observed at the weather station near to the irrigated area. However a large gap in the data was found for the year 2011-2012 seasons due to an

[1] http://data-portal.ecmwf.int/data/d/interim_full_daily/

operational error in the sensor. This was filled by the data downloaded from the ECMWF site. On close examination and observation it was observed that the distribution of both the satellite derived ECMWF data and the observations did not match. One of the reasons was that the temporal resolution of ECMWF was of three hours while for the observations it was one hour. The matching of the distributions was done through CDF matching technique (Choi & Jacobs, 2008; Reichle & Koster, 2004)

The Cumulative Distribution Function matching technique is used to reduce the bias between the ECMWF data and the measured ones. Here it uses the measured air temperature data at the station for the periods available and tries to reduce it's mismatching with that of ECMWF data. The CDF distribution and the bias for ECMWF and field measurements can be seen in Figure 4-6.

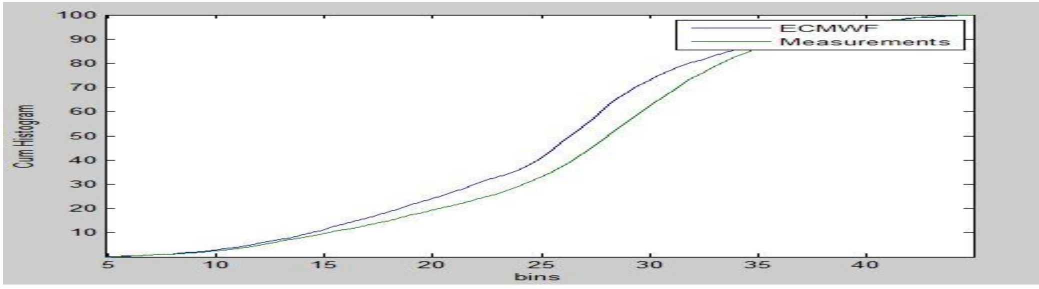

Figure 4-6 Cumulative histogram for ECMWF and MEASURED data, showing their bias.

The bias between the two data sets was most at the maximum and minimum daily temperatures. Henceforth the mean variations between two consecutive ECMWF data is obtained.

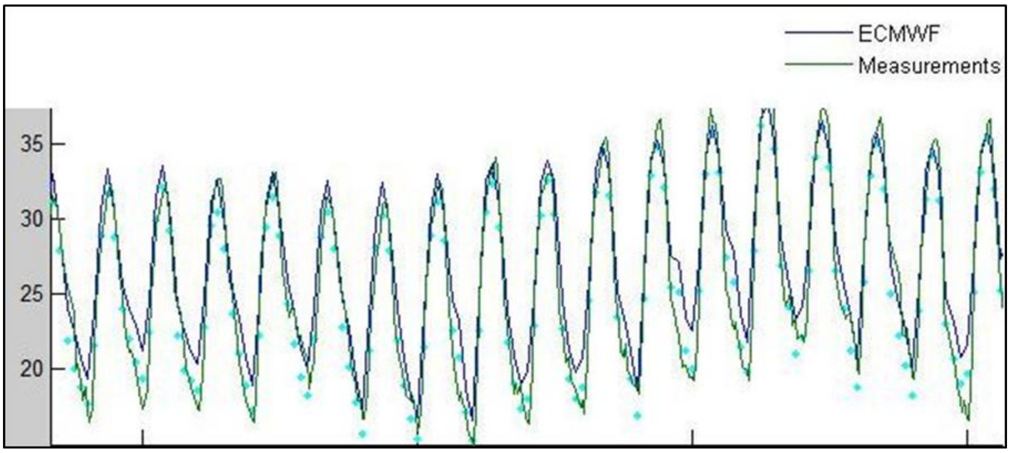

Figure 4-7 Matching of ECMWF data with the measured ones.

Once the CDF matching is done the shifting of the ECMWF values towards the observed values can be observed in Figure 4-7.

One of the important parameters in SCOPE are the soil boundary resistance (*rbs*), between the soil surface and the mean surface flow height (Villagarcía et al., 2007) and soil surface resistance (*rss*) (CAMILLO & GURNEY, 1986) a resistance as a function of soil moisture. The values of '*rss*' can be fixed since the insitu moisture conditions at the AOI pixel is known but this is not the case with '*rbs*' . considering the limits of '*rbs*' and arbitrary valueof 100 is considered. This arbitrary value of *rbs*, as 100 breeds uncertainties into the quantification of the energy balance components. This calls for a sensitivity analysis to be done to understand the extent of change of the energy balance components when rbs is varied between -80% and 100% from its arbitrary value of 100. The sensitivity analysis was carried out considering the difference between the maximum and the minimum value of the particular energy balance component at the time of satellite pass, (ToP) and when it was at its peak during the day.

4.1.4. Validation of High resolution ETa with SCOPE

Validation of the high resolution ETa obtained from step 3 is done with the ETa obtained from SCOPE. The validation of the high resolution ETa is done only for wheat because the field data was collected is only for the wheat. From Figure 4-5 we can observe that area covered by wheat constitutes a substantial part of the pixel.

4.1.5. Estimating water requirement.

The water requirements for the irrigated area are estimated taking into consideration the daily water status at the AOI. The procedure is explained in paragraph 2.4.

4.1.6. ETa based Performance evaluation of the irrigated area.

The main aim of performance assessment of the irrigated area is to understand its performance based on ETa estimates. This will help the policy planners and field engineers to evaluate on how close is the irrigated area to an ideal one. This information is important at the policymaking, operational and diagnostic levels. The ETa based performance indicators used in this study are given in paragraph 2.5. The level of performance guides the field engineer to understand if the irrigated area is performing good or bad or it is in the transition phase as shown in Figure4-8.

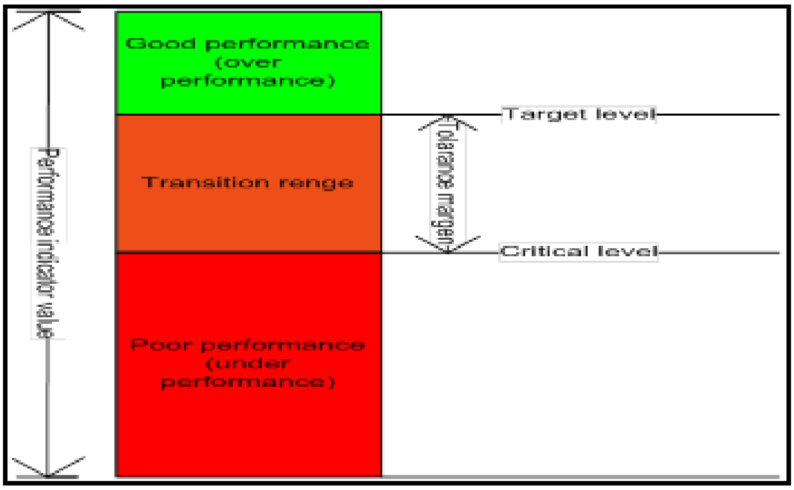

Figure 4-8 Target levels to assess the performance of an irrigated area.

4.2. Field data

4.2.1. Field measurements

The field data was collected from the AOI pixel in the irrigated area shown in Figure 1-1. The meteorological data was collected from the automatic weather recording station at SamHiggon Bottom Institute of Agriculture Technology and sciences, for the crop growing periods of 2010-11 and 2011-12. The LAI, soil moisture and the height of vegetation was collected on a decadal basis while the atmospheric vapour pressure in hPa, air temperature in ^{0}C and the wind velocity in ms^{-1} is obtained on a daily basis. Gaps were observed in the air temperature for the year 2011-12 and were filled by downloading these values form ECMWF site. However Cumulative Distribution Function Matching (CDF) matching was done to match them with the data for available days. The incoming shortwave and longwave incoming radiation was downloaded from ECMWF site.

4.2.2. Leaf Area Index

The Leaf Area Index (LAI, m^2m^{-2}), is used to monitor and assess the growth and vigour of the vegetation. The LAI of wheat crop grown in the AOI pixel was observed for both years of the crop growing seasons. The difference in LAI for both the years, as seen in Figure 4-9, is due to the difference in the sowing dates. Whereas we observe that it is almost the same at the end of the cropping period.

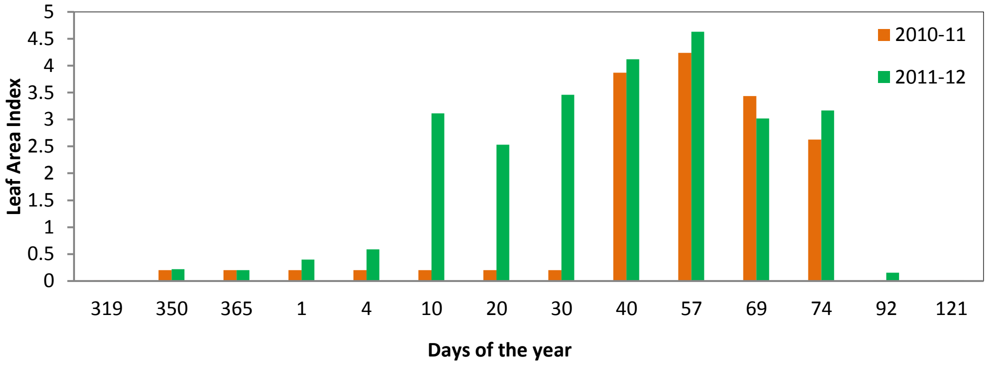

Figure 4-9 Leaf Area Index of wheat crop grown in the AOI pixel.

4.2.3. Plant height

The plant height of the wheat crop grown in the AOI, pixel was observed for both the crop growing seasons of the years 2010-11 and 2011-2012. The maximum height of the crop observed for both the years was about 0.6m. The difference in the planting height of wheat crop for both the years is due to the difference in the sowing dates. This can also be seen form Figure 4-10.

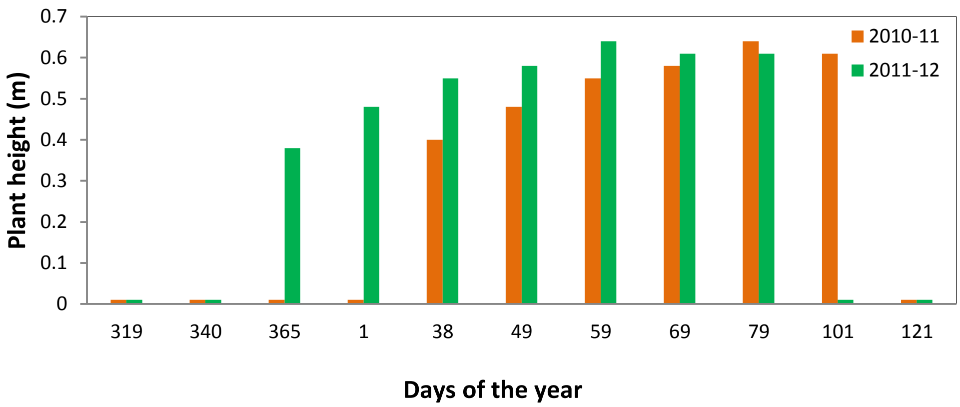

Figure 4-10 Height of the wheat crop at in the AOI pixel.

4.2.4. Soil moisture

The soil moisture at the AOI pixel was monitored throughout the crop growing seasons for the years 2010-11 and 2011-2012. The moisture in the AOI pixel depends upon the water released in the fields through the passing canal. The moisture level in the AOL pixel before and after cropping season remains about 0.1 m^3m^{-3}. From Figure 4-11 we can observe that the time of release of water from the canal into the irrigated area differs for both the seasons and its effect on crops can be seen from the previous figures.

The release of water or the availability of water at the farmer's field decides the dates for sowing of the crop.

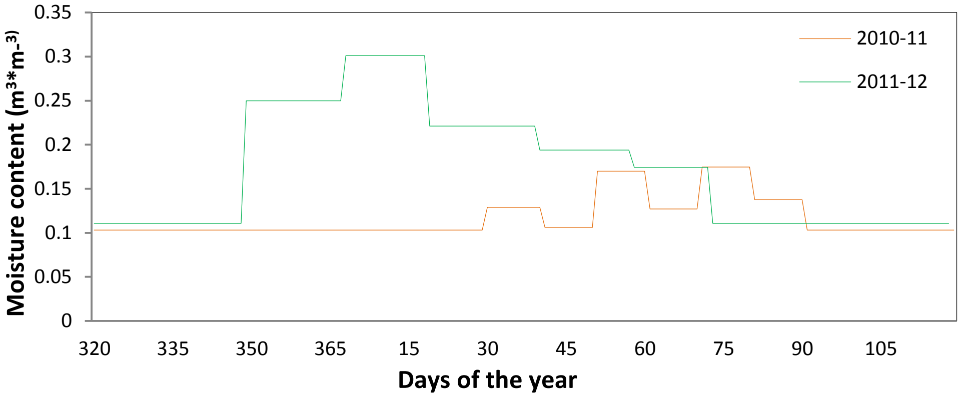

Figure 4-11 In-situ soil moisture at the AOI pixel.

4.2.5. Air temperature

The air temperature over the AOI pixel for the year 2010-11 from the station and the corrected ECMWF for the year 2011-12 is shown in Figure 4-12.

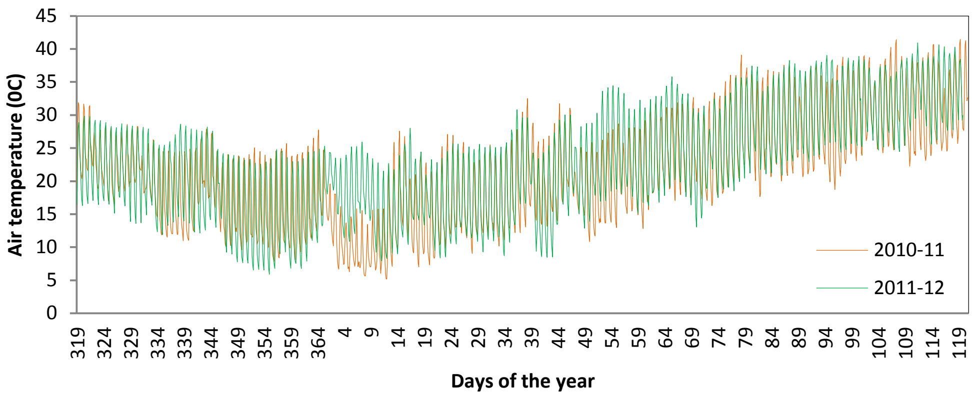

Figure 4-12 Air temperature over the AOI pixel.

4.2.6. Wind velocity

The wind velocity over the AOI pixel is shown in Figure4-13.

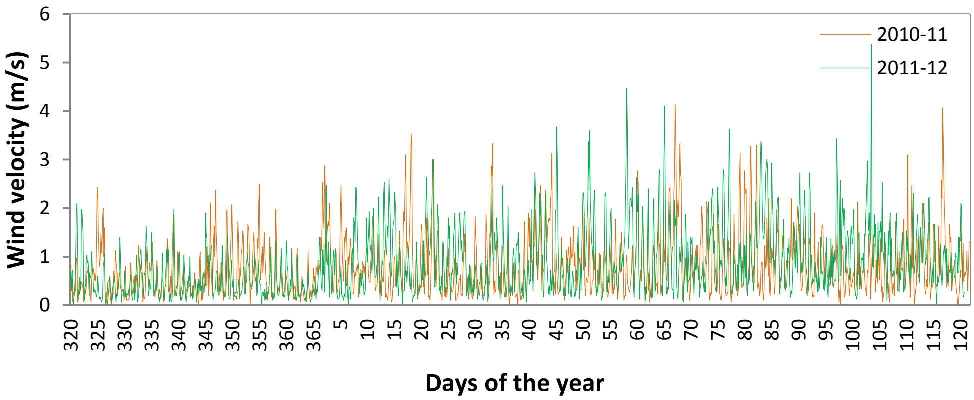

Figure 4-13 Wind velocity at the AOI pixel.

4.2.7. Incoming shortwave and longwave radiation

The instantaneous incoming shortwave radiation [W m^{-2}], comprises of the direct solar beam and scattered diffused part of the radiation that is received from the sun by the horizontal plane on the earth's surface per unit area. The incoming shortwave radiation over the AOI pixel is shown in Figure 4-14. This data is downloaded from ECMWF site.

The incoming longwave radiation [W m^{-2}], received on the surface of the earth, depends upon the vertical distribution of temperature, water vapour content and the concentration of carbon dioxide and ozone in the atmosphere. The longwave radiation received from the clear sky originates from the first few hundred meters of the atmosphere

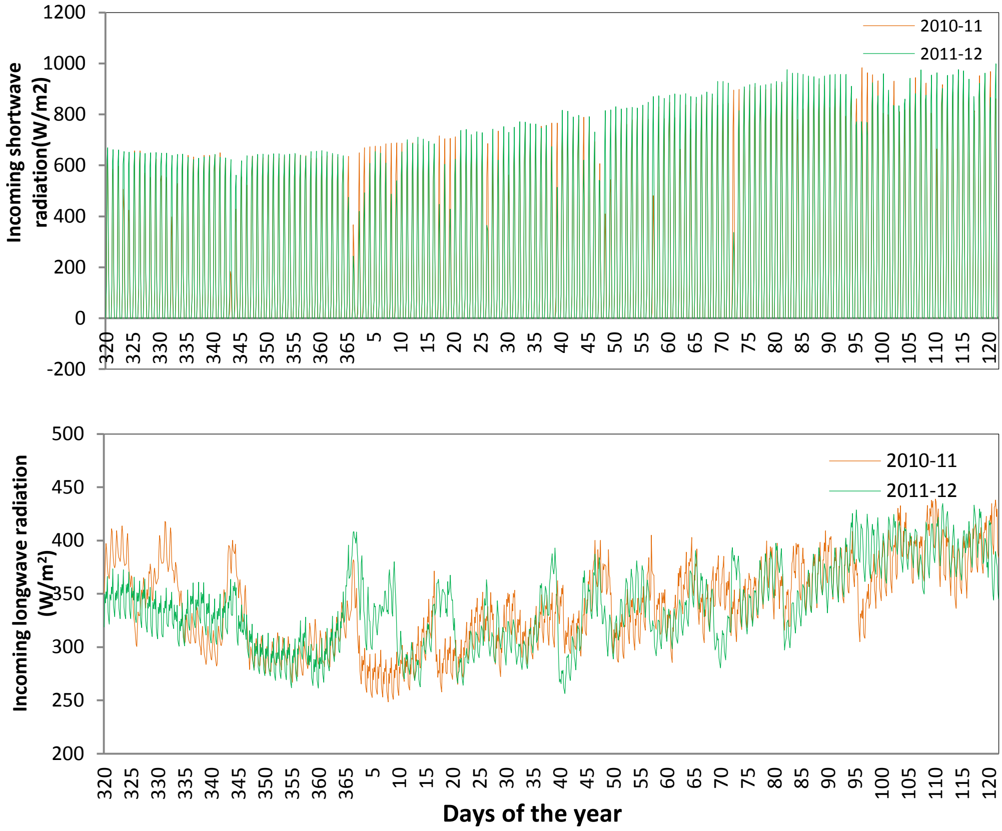

Figure 4-14 Incoming radiation over the AOI pixel.

In the above panel shortwave radiation is shown and in the bottom panel the longwave radiation is shown. The radiation over the AOI pixel has been downloaded from the ECMWF site.

4.2.8. Sunshine hours

The sunshine hours over the AOI pixel is shown in Figure 4-15. The total number of sunshine hours for the crop rowing season of 2010-11 was 1380 hrs, while for 2011-12 it was 1352 hrs.

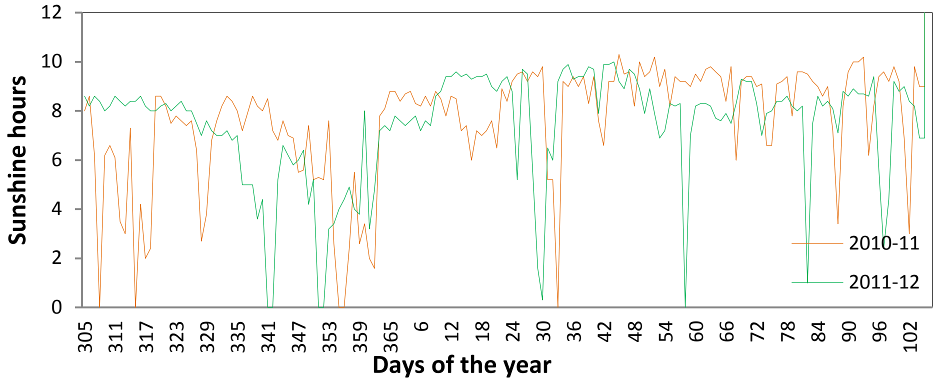

Figure 4-15 Sunshine hours over the AOI pixel.

4.3. Remote sensing data

The use of satellite data in quantifying important crop parameters such as ETa and plant growth is already an established fact (Allen et al., 1998.). The remote sensing data for period of observation for 2010-11 and 2011-12 was downloaded from ECMWF climate site. The downloaded data is shown in Table 4-3.

Table 4-3 Remote sensing meteorological data downloaded from ECMWF site.

Boundary layer height	m
Surface pressure	Pa
Mean sea level pressure	Pa
Surface solar radiation downwards	w/m^2
Surface thermal radiation downwards	w/m^2
Dew point temperature	K
Surface net solar radiation, clear sky	w/m^2

The MODIS data consisting of Land surface temperature/emissivity, NDVI, LAI, albedo and land cover was downloaded from the link [2].

Table 4-4 MODIS products and their specifications.

MODIS products	Product ID	Temporal resolution	Spatial Resolution (Km)
LST/emissivity	MOD11A1	Daily	1
NDVI	MOD13A2.5	16 days	1
LAI	MCD15A2	8 days	1
Albedo	MCD43B3.5	16 days	1
Land cover	MOD11A1	Yearly	1

The MODIS Terra products are used to asses the actual evaporation over the irrigated area. The MODIS HDF products are tiled in grids of 10^0 by 10^0. The orientation of each tile can be located by it's horizontal and vertical coodinates. The horizontal coodinates are from 0 to 35 while that of vertical from 0 to 17. The irrigated area having the AOI pixel is orientedlocated at the H25:V6 coodinates. Figure 4-16 shows

[2] http://modis.gsfc.nasa.gov/

the exact location of the study area marked with the red star. The MODIS products were downloaded from the following link:

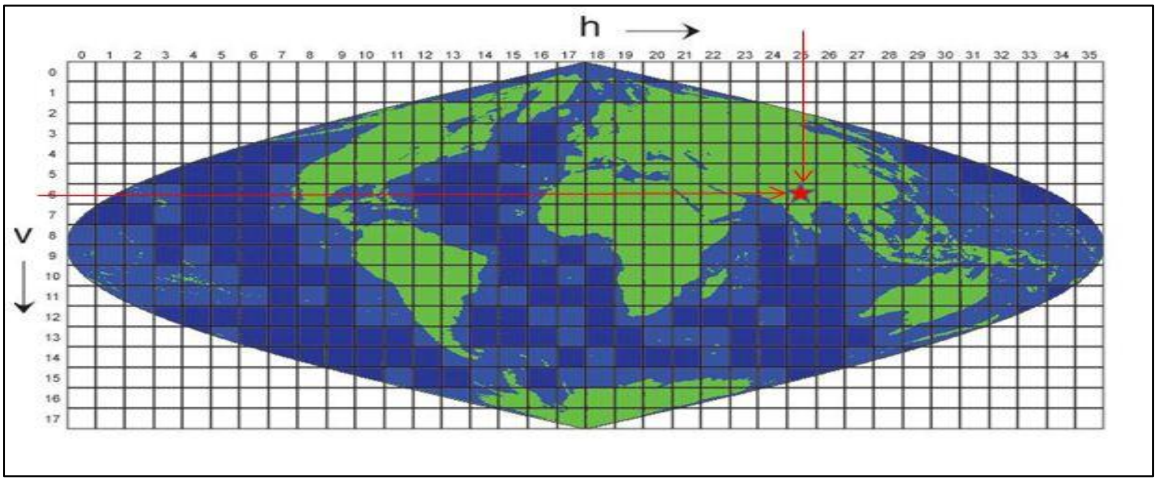

Figure 4-16 Tile selection for MODIS, H25:V6[3]

[3] http://e4eil01.cr.usgs.gov:22000/WebAccess/drill?attrib=home&next=group

5. RESULT AND DISCUSSION

This chapter deals with the results obtained using the theory explained in Chapter 2 and the methodology described in Chapter 3. It discusses in detail the results of SCOPE and SEBS in the terms of ETa along with the upscaled Eta and its validation. Further it assesses the irrigated area using ETa based performance indicators.

5.1. Actual evapotranspiration at regional scale using SEBS.

Evapotranspiration at regional scales is essential to quantify to understand the balance between the recharge and discharge from aquifers. Accurate estimates of ETa are needed when these measurements are to be used at a regional scale to manage water resources especially for scheduling irrigation for a large irrigated area. The ETa estimates are obtained for the winter crop growing seasons for the years 2010-11 and 2011-12. The ETa over the irrigated area is shown in Figure 5-1, along with the area of interest pixel.

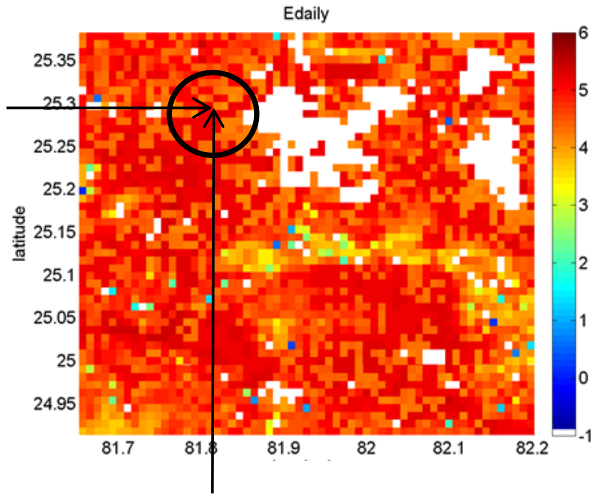

Figure 5-1 ETa estimates over the Irrigated area. The arrows show the area of interest pixel.

5.1.1. Evapotranspiration estimates over the irrigated area.

The ETa estimates for cloud free days, over the AOI pixel obtained using SEBS is shown in Figure 5-2 and 5-3.

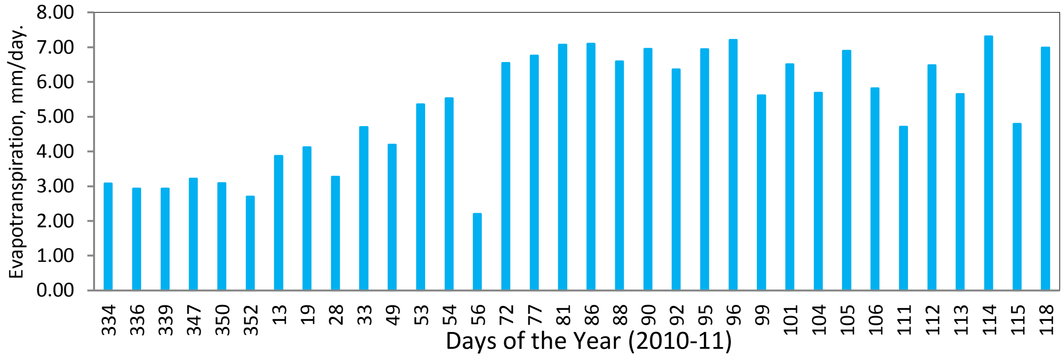

Figure 5-2 Evapotranspiration estimates over the AOI pixel for 2010-11

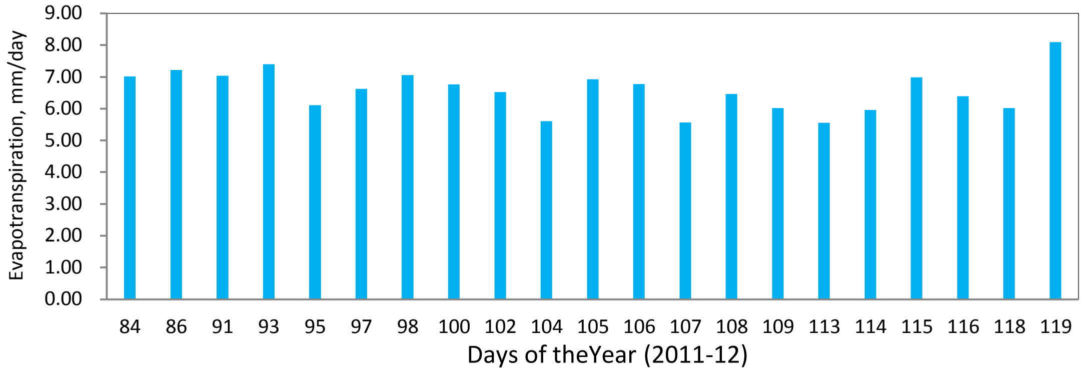

Figure 5-3 Evapotranspiration estimates over the AOI pixel for 2011-12.

The SEBS generated ETa for the entire irrigated area is shown in Figure 5-4. Upscaling of SEBS generated ETa has been done for the area of interest pixel, (AOI) that is situated in the centre of the irrigated area. The AOI pixel consists of eight classes all together. They are namely wheat, orchards, small vegetables, tubers, legumes, bare soil water and settlements. The SEBS ETa is disaggregated and ETa for individual land cover based upon the crops grown has been generated as shown in Figure 5-5. The results obtained for day 49 year 2010-11 are compared with that of SEBS. The AOI pixel is positioned at 81.81N and 25.3E. Similar results were obtained for the year 2011-12. Similarly the ETa for all the land cover classes are generated and shown in Figure5-6.

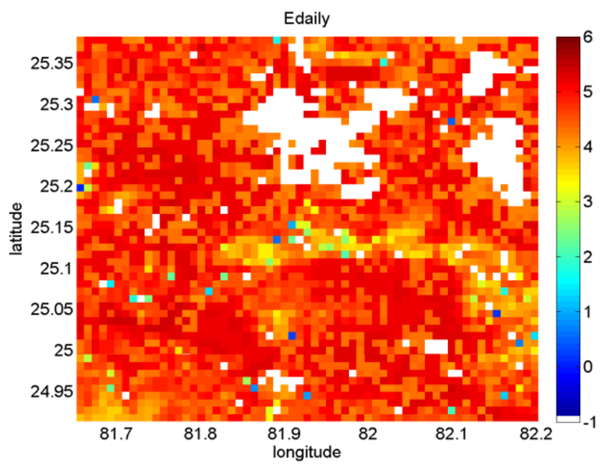

Figure 5-4 ETa estimates over the irrigated area for the day 49, 2010-11

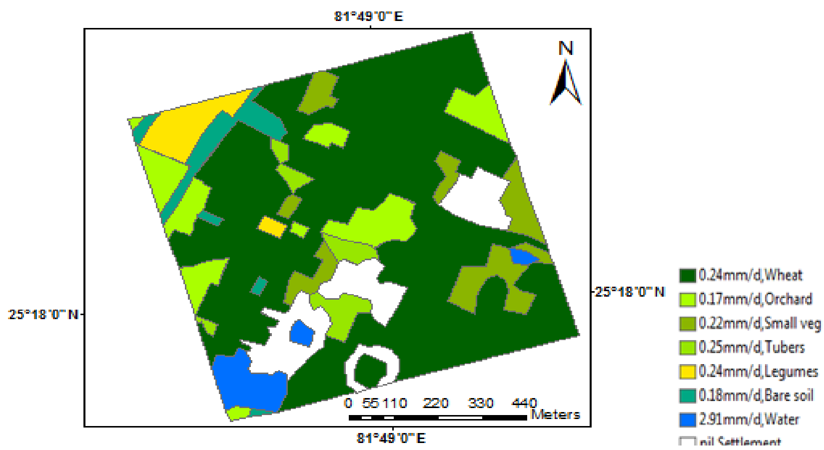

Figure 5-5 ETa estimates for the AOI pixel in the irrigated area for day 49, 2010-11

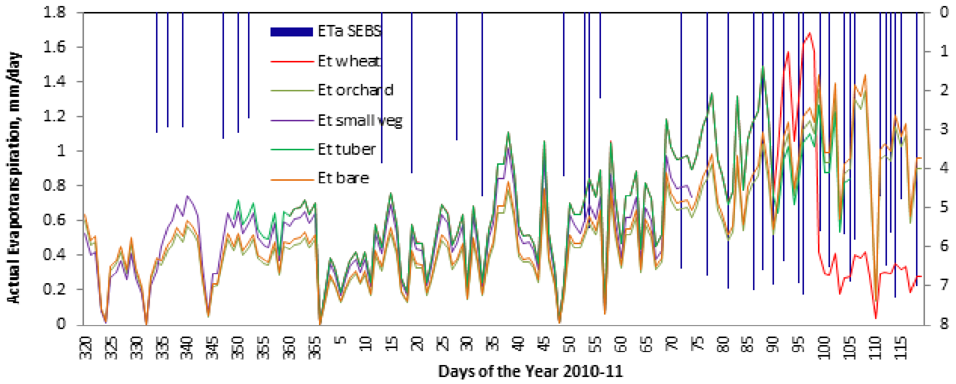

Figure 5-6 Upscaled and disaggregated SEBS ETa over the AOI pixel for the year 2010-11

5.2. Actual evapotranspiration at plot scale using SCOPE.

The estimation of ETa, at a plot scale stands important taking into consideration the size of agricultural plots in the irrigated area, as shown in Figure 1-1. SCOPE integrates the radiative transfer and energy balance calculations and is used here as a ground truth to validate upscaled ETa. The model simulates the ETa for wheat crop for the crop growing seasons of 2010-11 and 2011-12.

5.2.1. Actual evapotranspiration for wheat during cropping period of 2010-11-12.

The ETa, obtained for wheat for this crop growing season is shown in Figure 5-7. The wheat crop is sown in late December and is harvested in first week of April. The cropping dates depend upon the availability of moisture in the soil. For this year the soil moisture conditions were favourable due to the winter rains.

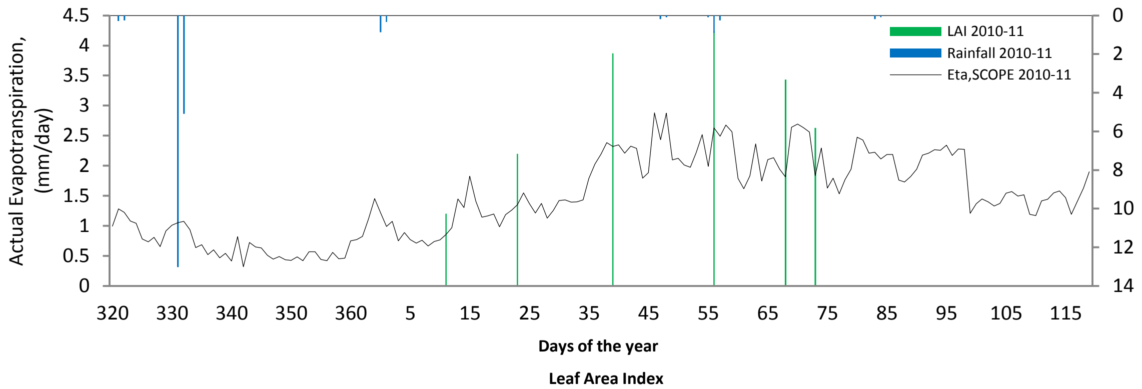

Figure 5-7 Actual evapotranspiration estimated by SCOPE from wheat for the crop growing period of 2010-11

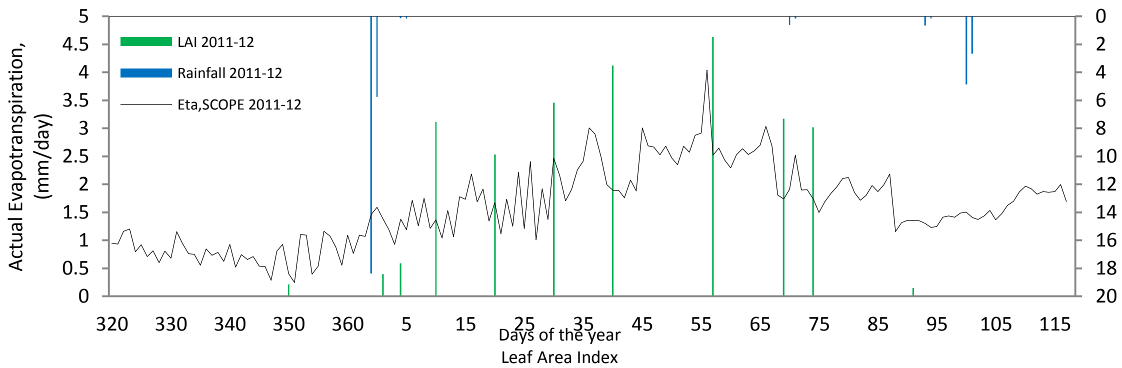

Figure 5-8 Actual evapotranspiration estimated by SCOPE for wheat for the crop growing period of 2011-2012.

The ETa obtained for wheat for the crop growing season of 2011-12 is shown in Figure 5-8. Both the figures show the increase in ETa along with the increase in LAI and vice versa.

The crop growth period has been divided into four regimes.

1) When the soil contains moisture following the monsoon rains and the agricultural plots are ready for the primary operations. At this stage LAI is negligible.
2) This is the crop sowing and growing stage. This period extends till the last irrigation. The LAI in this stage increases.
3) During this period the soil does not require additional moisture, moisture in the soil starts reducing and the plant is ripening. In this stage the LAI reaches its peak and gradually reduces as the crop ripens. This continues till the crop is harvested.
4) The last stage is after the harvest the plot is left bare with very little moisture.

The results exhibited here take into consideration the soil boundary resistance (*rbs*), between the soil surface and the mean surface flow height (Villagarcía et al., 2007) and soil surface resistance (*rss*) (CAMILLO & GURNEY, 1986) a resistance as a function of soil moisture. If the resistance at soil boundary increases, less water vapour is released into the atmosphere and the air surrounding the canopy gets warm hence increasing the sensible heat flux. At this stage the sensible heat flux dominates and heat is transferred into the air. The movement of moisture from the soil into the plant and through the stomata into the atmosphere depends mostly on the amount of moisture present in the soil and is a function of *rss*. More the moisture, less the *rss* and more the release of water into the soil boundary. More moisture in the soil leads to more absorption of the energy and has a direct effect on the Ground Heat flux. If the heat is absorbed into the soil the Ground Heat flux is positive and if it releases the heat it's negative.

Since the insitu soil moisture conditions are known, the values for *rss*, have been categorized into four. 350 for ideal condition, 1000 at the end of the last irrigation that is during crop ripening stage, 1200 before the sowing. This moisture is good for preparing the field for ploughing and 2000 for fully dry soils with very low moisture (C. van der Tol et al., 2009). The value of *rss,* ranges from 200 for considerably wet soil to 2000 for considerably dry soil. The values of *rbs*, is not known and hence a arbitrary value of 100 is considered. The range of *rbs*, at a maximum is considered at 200 while at a minimum it can be at 10 (C. van der Tol et al., 2009). The results obtained for both the crop growing years 2010-11 and 2011-12 are shown and discussed below.

5.2.1.1. Sensitivity analysis for the Net radiation.

The net radiation (Rn) is not sensitive to the change is *rbs*. This is due to the fact that Rn, depends upon the incoming solar radiation which is independent of the crop or soil properties. The Figure 5-9 very clearly exhibits this property of the net radiation. This will only vary when there is a cloud cover over the irrigated area or the AOI pixel.

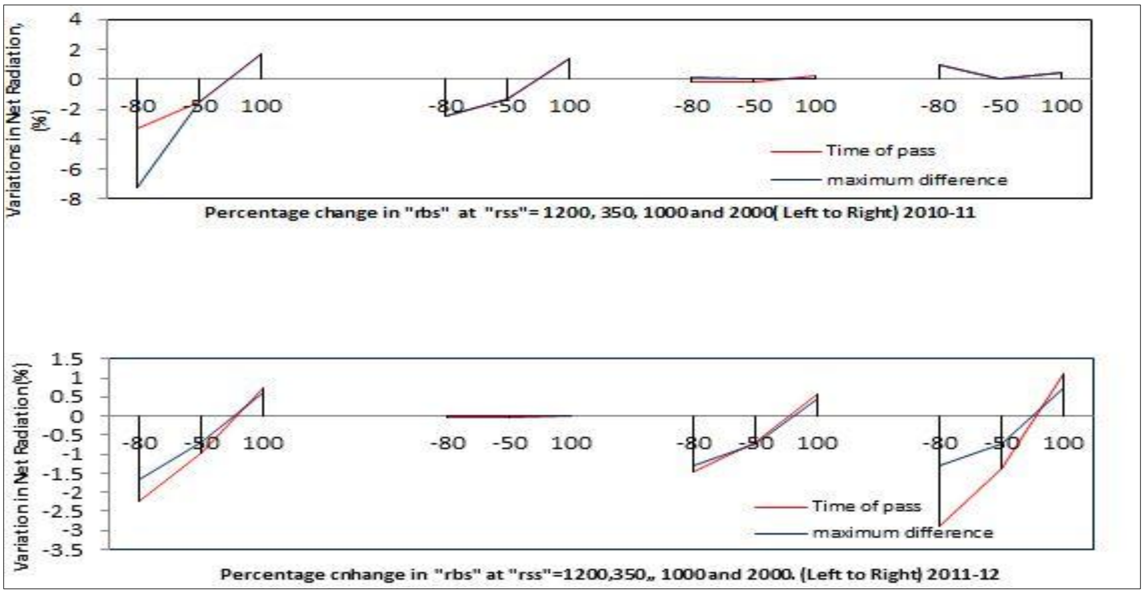

Figure 5-9 Extent of uncertainties in Net Radiation with respect to changes in "rbs".

5.2.1.2. Sensitivity analysis for Latent Heat.

The sensitivity analysis for the Latent Heat, λE is shown in Figure 5-10. In the year 2010-11 moisture is released in the soil at a later date as shown in Figure 4-11. It is observed that for a *rss* of 350, at ToP, the maximum variation is about 30% as the *rbs* is reduced by 80%. An increase in *rbs* increases the release of moisture into the boundary surface and thus increases the λE. At a *rss* of 1200 and 2000 when the soil is bare the variations are almost the same as *rbs* is increased or decreased, clearly indicating the non-availability of a canopy in the soil boundary layer. The variations in λE was observed to be the least at an *rss* of 1000. This is the stage when the canopy is the densest and any change is rbs does not affect the λE. The sensitivity analysis for the year 2011-12 shows that the λE is not sensitive to the any change in *rbs* at a *rss* of 1200, 350 and1000. This is due to the fact that during this period there is sufficient moisture in the soil. This can be verified form Figure 4-11 also. As for a *rss* of 2000, as the moisture reduces the variations again can be observed especially during the day time. Similar results are exhibited by(Mallick et al., 2013)

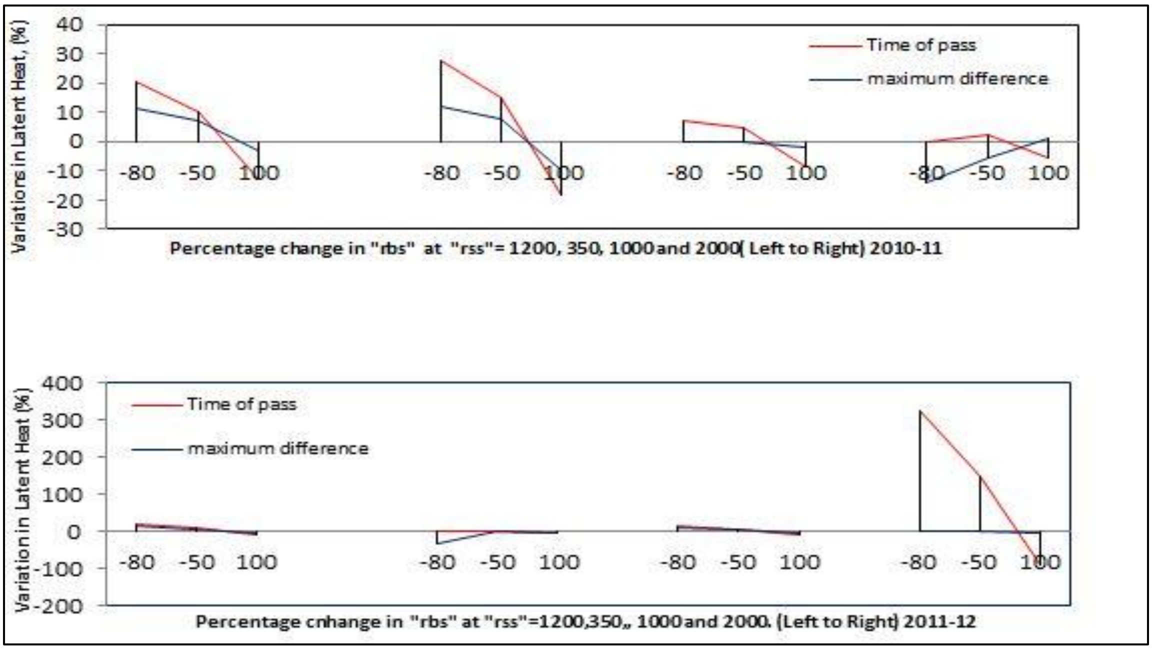

Figure 5-10 Extent of uncertainties in Latent Heat with respect to change in "rbs".

5.2.1.3. Sensitivity analysis for Sensible Heat.

During dry conditions when the evaporation becomes limiting, the incoming energy is dissipated through the Sensible Heat (H), which results in a rise of air temperature. With an increase in *rss*, less moisture will be released into the boundary layer. When this condition is coupled with an increase in *rbs*, the variations are going to be minimized as it leads to heat up the already heated air. A decrease in *rbs* will certainly help the hot air to rise and thus create variations in the H values. For the year 2010-11 it is observed that for a *rss* of 1200 and 2000 when the soil is bare, the trends in variation of “H” is same except for the magnitude. This is due to the difference in moisture levels. A *rss* of 1200 releases more moisture than a *rss* of 2000. At a *rss* of 1000 a variations of 50% in H is observed. During this period the thick canopy of the crop plays a major role and over comes the effect of a change in the *rbs* within the considered range. The observations made during the crop growing season of 2011-12 very clearly show the effect of crop growth on the variations of H. This year the crop is grown early due to availability of water in the canal. For a *rss* of 1200 and 350 the variations remain at 50% within the whole range of *rbs*. At a rss of 1000 and at the ToP the variation observed is found to be at a extent of 350%. This may be due to observation of the incoming solar radiation considered during cloudy days. The variation in the H values during the remaining part of the day show minimum variation within the range of *rbs*. In dry and bare soil at a *rss* of 2000 for the same year, H is not sensitive for rbs values at the ToP, while exhibits a high sensitivity during the remaining period. Similar results are obtained by (Mendina & Terra, 2012) in their study of sensitivity of simulated convection to soil moisture. This can be seen in Figure 5-11.

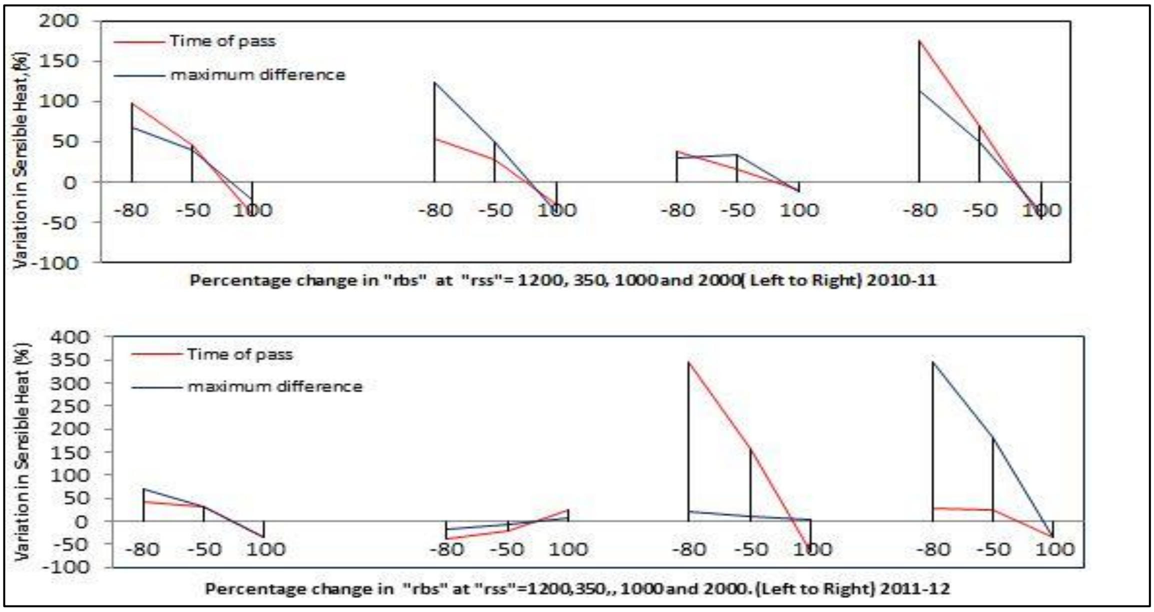

Figure 5-11 Extent of uncertainties in Sensible Heat with respect to change in "rbs".

5.2.1.4. Sensitivity analysis for Ground Heat.

The Ground Heat flux at the surface G, is defined as the rate of heat exchange between the earth surface and the soil below(Christiaan van der Tol, 2012). It is positive when it is in the downward direction and negative when is released in the atmosphere. The sensitivity analysis of G for the year 2010-11 and 2011-12 is discussed taking into consideration the results shown in Figure 5-12. The results reveal that for *rss* 1000 and 2000 the variations in G follow almost the same trend. The variations are minimum at *rss* 1200 when the soil is considerable moist and is bare. For the same *rss* values, in 2011-12, the variations in G follow the same trend. The wet the soil the more absorption of energy takes place as the wet soil has more conductance than the dry soil.

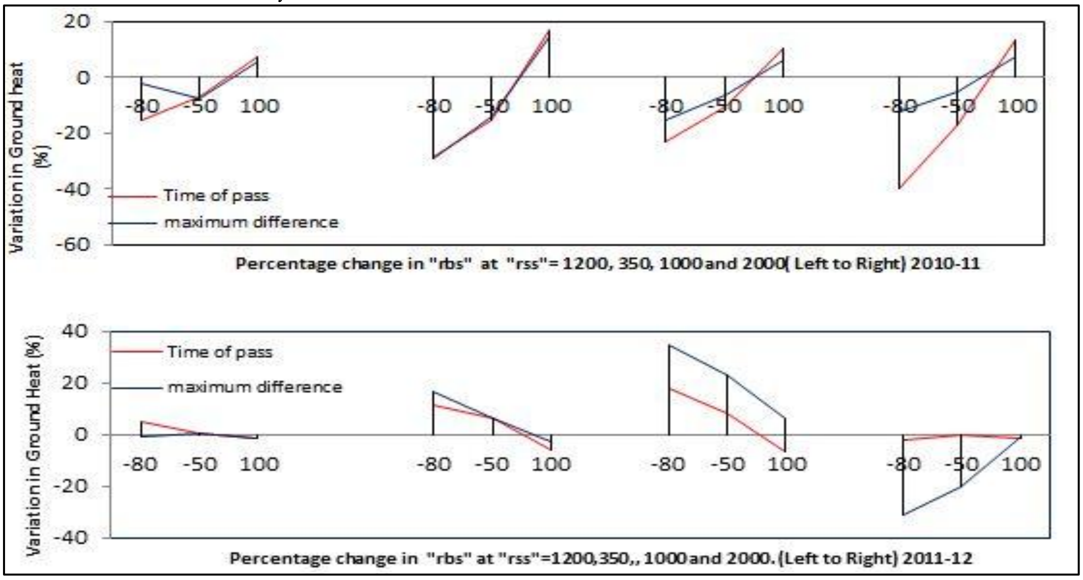

Figure 5-12 Extent of uncertainties in Ground Heat with respect to change in "rbs".

The λE estimates of SCOPE for the crop growing seasons of 2010-11 and 2011-12 does include uncertainties due to *rbs* estimates. These results describe the extent of uncertainties in each regime and give an estimate of the variations in the energy balance components and their impact on the ETa estimates.

5.3. Validation of upscaled ETa with SCOPE

The upscaled ETa is validated by the ETa generated by SCOPE. The ETa generated by SCOPE is considered as a ground truth and is used to validation the upsacled SEBS ETa. A comparison between SEBS generated low resolution ETa and upsacled ETa with that of SCOPE is done to understand the validity of the upscaled ETa. This validation is limited to the wheat crop only and is shown in Figure 5-13. The data required to validate with other crops was not available. The RMSE and MAE for correlation between SEBS (low resolution) and SCOPE was found to be 16.012 [mm day^{-1}] and 3.738. These values reduced to 1.18 [mm day^{-1}] and 0.967 in case of correlation obtained between upscaled SEBS ETa and that of SCOPE.

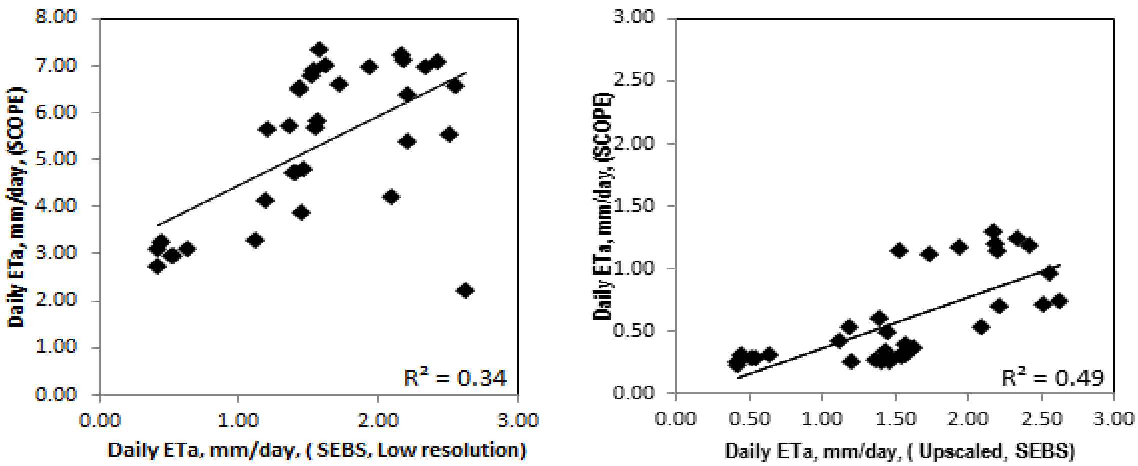

Figure 5-13 Validation of upscaled SEBS ETa for wheat with SCOPE, for the year 2010-11.

5.4. Assessment of irrigated area experiencing performance gaps,based upon ETa estimates.

The most important purpose of irrigating an agricultural area is to apply the intended volume of water to the crops to create optimum soil moisture conditions in the soil so as to avoid undesirable stress throughout the cropping period. Most of the water applied is released into the atmosphere as evapotranspiration while the remaining drains out. This makes regular assessment of the irrigated area important. This helps to identify period with water stress. Thus measures are taken to negate their effects. The time series of performance indicators plotted with respect to their critical or threshold values helps the field engineer to know when these values will be reached and accordingly management actions are taken. Water (being the most important input in plant growth) becomes limited due to evaporation from soil and crops, hence ETa based evaluation is performed for the irrigate area based upon upscaled ETa and the results are shown and discussed below. The irrigation requirements are calculated based upon the actual soil moisture status and the upscaled SEBS ETa, at the AOI pixel .

5.4.1. Delivery Performance Ratio.

Water measuring devices are not installed at the channels of the study area, supplying water to an irrigated area. Therefore time remains the only criteria to quantify the water delivery performance. The Delivery performance ratio (DPR) compares the actual water delivered to the intended. The DPR for the AOI pixel is calculated taking into consideration the water supplied to the AOI pixel and the intended flow of water into it. The target level of DPR is set at 0.8 while the critical level is at 0.6. A DPR of 1.0 is an ideal situation. If the DPR is more than 1.0 it indicates over irrigation and if it is below this level indicates moisture stress (Bandara, 2006). The DPR for the irrigated AOI pixel is shown in Figure 5-14.

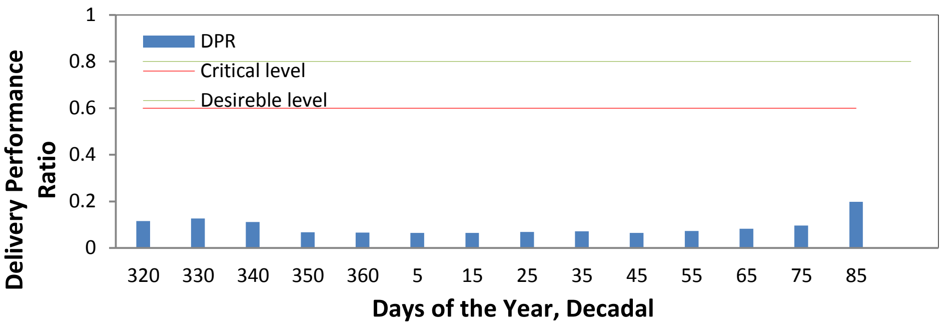

Figure 5-14 The Delivery Performance Ratio for the AOI pixel for the year 2010-11.

The water is released into the AOI on a decadal basis. The DPR remains critical throughout the growing season. This shows the scarcity of water throughout the cropping period. Wheat being the major crop uses more water. This can be seen by the reducing DPR as the crop grows. As the irrigation to wheat is stopped the remaining water is diverted for other crops, the DPR improves. A prolonged low DPR indicates needs for improvement in the existing management plans. While it also shows that the application of water in the region is uniform and scare at all irrigations.

5.4.2. Depleted Fraction.

The depleted fraction indicates the scarcity of water over the Gross Command Area (GCA) area. It compares three components of the water balance that are the water supplied for irrigation, the intended water supply and the precipitation over the area. This influences the decision of the water supply in the area. It is an indicator of the amount of water that is available for storage in the ground water. If the ETa is less than 0.6 of the sum of water supplied and rainfall over the irrigated area, a part of irrigated water goes into storage otherwise depletion of ground water takes place. This helps in understanding the water balance of the irrigated area. If water is stored in the GCA, less water may be diverted to the crops and if the ground water is depleting, more water can be used for irrigation.

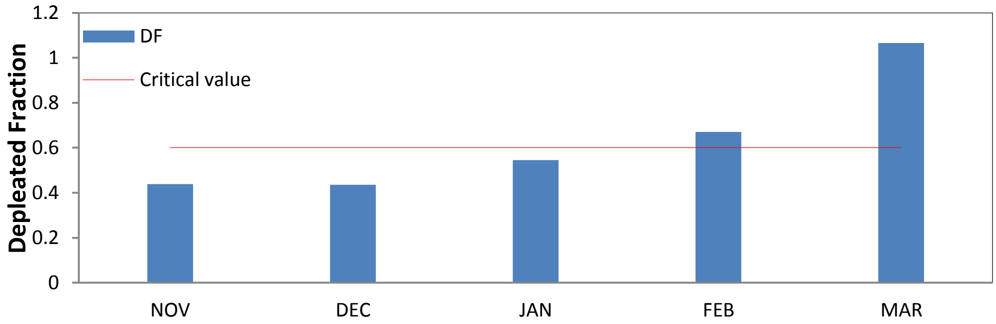

Figure 5-15 Monthly values of the Depleted Fraction over the AOI pixel for the year 2010-11

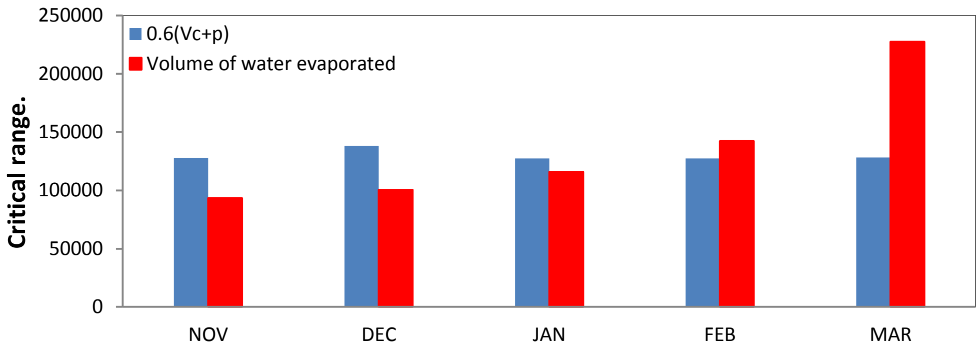

Figure 5-16 Water balance over the GCA having the AOI pixel for the year 2010-11.

As the ETa over the GCA increases more than the sum of irrigated water and rain the water starts depleting in the GCA. This is seen form Figure 5-15 and Figure 5-16.

5.4.3. Relative Evapotranspiration

Relative evapotranspiration helps us to understand the adequacy of irrigation water delivery over the irrigate area as a function of time (Awan et al., 2011). The water supply at during the months of December and January indicate the adequate water supply when the RET values are between 0.8 and 1. The RET remains below the desired levels for the month of November, February and March indicating the level of inadequacy in the AOI pixel. This can be seen from Figure 5-17.

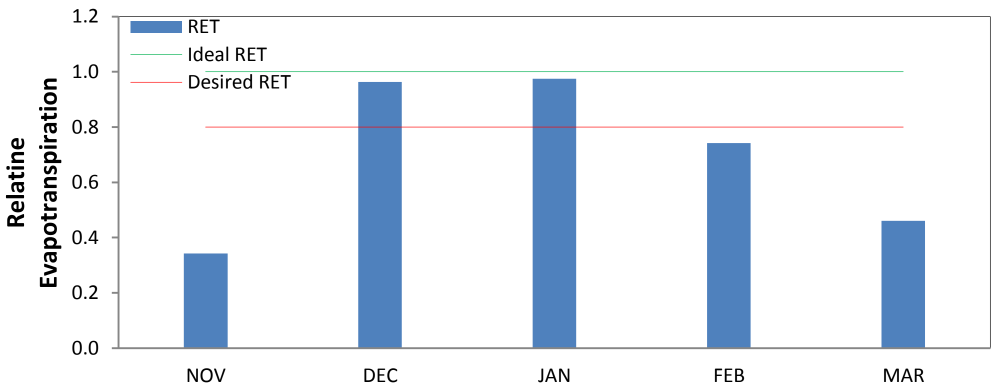

Figure 5-17 Relative Evapotranspiration over the AOI pixel for the year 2010-11

5.4.4. Crop Water Deficit

The crop water deficit is defined as the difference between the actual and potential evapotranspiration from an irrigated area. It indicates the water stress and water deficit in the irrigated area over a period of time. An average of CWD of 30mm/month is acceptable(M. G. Bos et al., 2005). The critical levels of CWD can be seen in Figure 5-18. The months of November, December and March remain critical were as the CWD is acceptable for the months of January and February

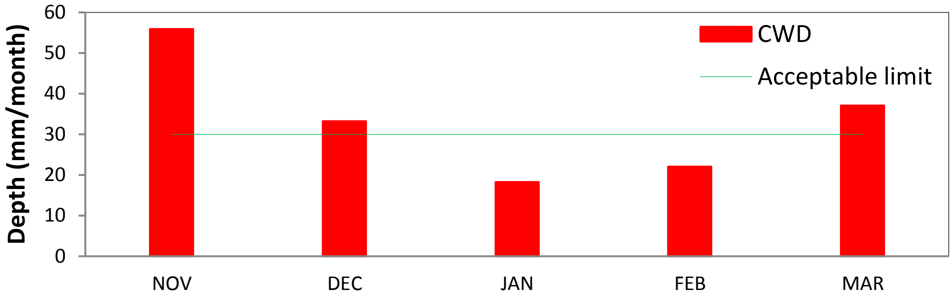

Figure 5-18 Crop Water Deficit for the wheat crop for the year 2010-11

6. SUMMARY AND CONCLUSION.

The total irrigated area covered by government sponsored canal networks in India is about 15.3 million ha. Nearly 81% of farm holdings are less than 1.33 ha. and cover 44% of the total CCA. Their contribution to GDP is immense. Hence it is essential to access and manage these small irrigated areas both spatially and temporally. Small irrigated lands are difficult to manage spatially. Remote sensing techniques hold good promise but rising cost of high resolution images negates it, while low resolution images are freely available.

This research tries to develop a cost effective method to assess an irrigated area with using low resolution, free of cost, MODIS images. This goal was broken down into several research questions:

1. Does the upscaling of SEBS increase comparisons with measurements or simulations of actual evapotranspiration?
2. How can the performance of an irrigated area be accessed by performance indicators based on ETa ?
3. What is the temporal variation of water stress in the irrigated area?
4. What should be the measures to reduce the uncertainties when measuring performance?
5. Does this experience produce practical recommendations to improve the performance of the irrigate area? What are they?

To answer the research questions, the following methodology was developed. SEBS was used to generate the ETa for the area at low resolution. Upscaling of low resolution SEBS ETa is done to get high resolution ETa. High resolution ETa for wheat was validated against SCOPE simulations for crop growing seasons of 2010-2011 and 2011-2012. Afterwards the high resolution ETa is used to evaluate the irrigated area using water balance indicators. The results reveal that this technique can be used to upscale low resolution images and addresses issue of adequacy and equity of water distribution in an irrigated area. It addresses all the research questions arising from the findings:

1) The ETa from SCOPE, low resolution SEBS and upscaled SEBS for wheat for the crop growing season of 2010-11 are compared. This comparison however could not be done for 2011-12 due to a large number of cloudy days. For the season 2010-2011 an increase in correlation was found; the correlations between low resolution SEBS and SCOPE was 0.32 which increases when comparing upscaled SEBS with SCOPE to 0.49. . The results for the year 2010-11 are quite encouraging as the RMSE was reduced by 14.83 [mm day^{-1}] and MEA by 0.96.
2) The performance of an irrigated area through remote sensing is based upon water balance estimates at the AOI pixel. ETa and ETp estimates over the AOI pixel have been obtained. Using ETa, the Delivery performance ratio, Depleted fraction, Relative evapotranspiration, and the Crop water deficit have been calculated. The results of these calculations show that
    a. The Delivery performance ratio is far below acceptable limits for the whole of the cropping period. Water supplied is less than the actual demand.
    b. The Depleted fraction is observed to be within the acceptable limits in the first three months of crop growth indicating a stability of the storage of soil water or ground water. This soil water or ground water is seen to be depleted in the months of February and March indicating a reduction in the water storage.
    c. A Relative evapotranspiration of 0.8 and below indicates that the crop is under stress. The RET obtained over the AOI shows prolonged water stress periods. The water stress period in this case covers the months of February and March.
    d. Crop water deficit was shown to be cross the critical level during January and February.

3) The temporal variation of water stress in the irrigated area was successfully shown for each performance indicator. The Delivery performance ratio indicates water stress all through the cropping period. The Relative evapotranspiration indicates water stress through the most of the irrigated period except, February and March. The Crop water deficit also indicated water stress for the most of the period, but indicates the safe limits for the same two months as that of Relative evapotranspiration.
4) The water balance indicators based upon ETa estimates do help in the assessment of an irrigated area. These ETa estimates however also include some uncertainties. These uncertainties can be reduced by taking into consideration the following:
    a) The meteorological station should be situated at the irrigated area.
    b) Time series measurements of insitu soil moisture status over the entire irrigated area.
    c) Regular ground water levels at the irrigated areas be measured to validate the DF.
    d) The frequency of estimating the water balance indicators
    e) The conveyance and water loss due to seepage must be considered.
5) For the recommendations the small plot size should be taken into consideration. As such the recommendations to improve the performance of the irrigated areas are as follows:
    a) The remote sensing technique developed proves to be very useful in the assessment of the irrigated area both on a high temporal and spatial resolution.
    b) The technique developed provides efficient solutions for managing small farm lands.
    c) Water supplied to the irrigated area should match the actual water demand.
    d) In case water or energy to pump this water is limited, deficit irrigation should be practiced. Water should be supplied to match the critical levels if not the desired levels.
    e) Water measurements must be considered at the point where the water moves out of the canal and not at the pump house. This becomes more important in case the canal is unlined, as it is in this case. This gives more realistic water measurements.
    f) To improve the DPR the inflow of water must be reduced in case of rainfall.
    g) The type of crop may be more homogeneous over the entire irrigated area. This will help in reducing uncertainties in ETa observations using medium or low resolutions remote sensing images.

A cost effective method to assess an irrigated area with using low resolution has been developed. Temporal and spatial assessment of an irrigated area using ETa, helps in understanding the issues of adequacy and equity of water supply. The method developed using SEBS and SCOPE synergistically successfully increases the precision of low resolution ETa. The water balance indicators using the high resolution ETa estimates are capable of assessing an irrigated area.

LIST OF REFERENCES

Ahmad, M.-u.-D., Stein, A., & Bastiaanssen, W. G. M. (2004). Estimation of disaggregated canal water deliveries in Pakistan using geomatics. *International Journal of Applied Earth Observation and Geoinformation, 6*(1), 63-75. doi: 10.1016/j.jag.2004.07.008

Allen, R. G., Pereira, L. S., Raes, D., & Smith, M. (1998.). Crop evapotranspiration, guidelines for computing crop water requirements., . *FAO Irrigation and Drainage paper 56*(Food and Agricultural Organization of United Nations (FAO) Rome, Italy), pp 300.

Anderson, M. C., Allen, R. G., Morse, A., & Kustas, W. P. (2012). Use of Landsat thermal imagery in monitoring evapotranspiration and managing water resources. *Remote Sensing of Environment*(0). doi: 10.1016/j.rse.2011.08.025

Awan, U. K., Tischbein, B., CConrad, Martius, C., & Hafeez, M. (2011). Remote Sensing and Hydrological Measurements for Irrigation Performance Assessments in aWater User Association in the Lower Amu Darya River Basi. *Water Resour Manage, 25*, 2467–2485.

Bandara, K. M. P. S. (2006). Assessing irrigation performance by using remote sensing. *ITC Dissertation 134* 86 - 87.

Bastiaanssen, W. G. M. (1995). Regionalization of Surface Flux Densities and Moisture Indicators in Composite Terrain: A Remote Sensing Approach Under Clear Skies in Mediterranean Climates.

Bastiaanssen, W. G. M., Menenti, M., Feddes, R. A., & Holtslag, A. A. M. (1998). A remote sensing surface energy balance algorithm for land (SEBAL). 1. Formulation. *Journal of Hydrology, 212–213*(0), 198-212. doi: 10.1016/s0022-1694(98)00253-4

Beljaars, A. C. M., & Holtslag, A. A. M. (1991). Flux Parameterization over Land Surfaces for Atmospheric Models. *Journal of Applied Meteorology, 30*(3), 327-341. doi: 10.1175/1520-0450(1991)030<0327:fpolsf>2.0.co;2

Bhumralkar, C. M. (1974). Numerical Experiments on the Computation of Ground Surface Temperature in an Atmospheric Circulation Model. *Journal of Applied Meteorology, 14*, 1246 - 1258.

Bos, M. G. (1997). Performance indicatiors for irrigation and drainage. *Irrigation and Drainage Systems, 11*, 119 - 137.

Bos, M. G., Burton, M. A., & Molden, D. J. (2005). Irrigation and drainage performance assessment: practical guidelines. *IWMI Books Reports, International Water Management Institute, , No H037064*.

Bos, M. G., Kselik, R.A.L., Allen, R.G., Molden, D. (2008). Water Requirements for Irrigation and the Environment.

BOS, M. G., WOLTERS, W., DROVANDI, A., & MORABITO, J. A. (1991). The Viejo Retamo secondary canal, Performance evaluation case study." Mendoza, Argentina. *Irrigation and Drainage Systems 5*, 77-88.

Briscoe, J., & Malik, R. P. S. (2005). India's Water Economy: Bracing for a Turbulent Future. India, New Delhi: Oxford University Press,World Bank.

Brutsaert, W. (1999). Aspects of bulk atmospheric boundary layer similarity under free-convective conditions. *Rev. Geophys., 37*(4), 439-451. doi: 10.1029/1999rg900013

CAMILLO, P. J., & GURNEY, R. J. (1986). A Resistance Parameter for Bare-Soil Evaporation Models. *Soil Science, 141*(2), 95-105.

Cammalleri, C., Ciraolo, G., La Loggia, G., & Maltese, A. (2012). Daily evapotranspiration assessment by means of residual surface energy balance modeling: A critical analysis under a wide range of water availability. *Journal of Hydrology, 452*, 119-129. doi: 10.1016/j.jhydrol.2012.05.042

Choi, M., & Jacobs, J. (2008). Temporal Variability Corrections for Advanced Microwave Scanning Radiometer E (AMSR-E) Surface Soil Moisture: Case Study in Little River Region, Georgia, U.S. *Sensors, 8*(4), 2617-2627.

Clemmens, A. J., & Bos, M. G. (1990). Statistical methods for irrigation system water delivery performance evaluation. *Irrigation and Drainage Systems, 4*, 345 - 365.

Cuevas, M. V., Torres-Ruiz, J. M., Álvarez, R., Jiménez, M. D., Cuerva, J., & Fernández, J. E. (2010). Assessment of trunk diameter variation derived indices as water stress indicators in mature olive trees. *Agricultural Water Management, 97*(9), 1293-1302. doi: 10.1016/j.agwat.2010.03.011

CWC. (2011). Annual Report, Ministry of Water Resource , Government of India.

de Fraiture, C., Molden, D., & Wichelns, D. (2010). Investing in water for food, ecosystems, and livelihoods: An overview of the comprehensive assessment of water management in agriculture. *Agricultural Water Management, 97*(4), 495-501. doi: 10.1016/j.agwat.2009.08.015

FAO 56. (1998). Crop evapotranspiration guidelines for computing crop water requirements. *FAO Irrigation and Drainage paper 56*.

Gupta, S. K., & Deshpande, R. D. (2004). Water for India in 2050: first-order assessment of available options. [REVIEW ARTICLE]. *CURRENT SCIENCE, VOL. 86* (NO. 9), 1216-1224.

Ha, W., Gowda, P., & Howell, T. (2012a). A review of downscaling methods for remote sensing-based irrigation management: part I. *Irrigation Science*, 1-20. doi: 10.1007/s00271-012-0331-7

Ha, W., Gowda, P., & Howell, T. (2012b). A review of potential image fusion methods for remote sensing-based irrigation management: part II. *Irrigation Science*, 1-19. doi: 10.1007/s00271-012-0340-6

Howell, T. A., & Evett, S. R. (2011). The Penman-Montheith Method http://www.cprl.ars.usda.gov/pdfs/PM%20COLO%20Bar%202004%20corrected%209apr04.pdf.

Hwang, T., Song, C., Bolstad, P. V., & Band, L. E. (2011). Downscaling real-time vegetation dynamics by fusing multi-temporal MODIS and Landsat NDVI in topographically complex terrain. *Remote Sensing of Environment, 115*(10), 2499-2512. doi: 10.1016/j.rse.2011.05.010

Jacquemoud, S., Verhoef, W., Baret, F., Bacour, C., Zarco-Tejada, P. J., Asner, G. P., . . . Ustin, S. L. (2009). PROSPECT;SAIL models: A review of use for vegetation characterization. *Remote Sensing of Environment, 113, Supplement 1*(0), S56-S66. doi: http://dx.doi.org/10.1016/j.rse.2008.01.026

Joshi, P. K., & Tyagi, N. K. (1994). Salt affected and waterlogged soils in India: a review. In: Svendsen, M., Gulati, A. (Eds.) Strategic Change in Indian Irrigation.ICAR, New Delhi, and IFPRI, Washington, DC, USA. 237–252.

Kalma, J., McVicar, T., & McCabe, M. (2008). Estimating Land Surface Evaporation: A Review of Methods Using Remotely Sensed Surface Temperature Data. *Surveys in Geophysics, 29*(4-5), 421-469. doi: 10.1007/s10712-008-9037-z

Kim, G., & Barros, A. P. (2002). Downscaling of remotely sensed soil moisture with a modified fractal interpolation method using contraction mapping and ancillary data. *Remote Sensing of Environment, 83*(3), 400-413. doi: 10.1016/s0034-4257(02)00044-5

Knox, J. W., Kay, M. G., & Weatherhead, E. K. (2012). Water regulation, crop production, and agricultural water management—Understanding farmer perspectives on irrigation efficiency. *Agricultural Water Management, 108*(0), 3-8. doi: 10.1016/j.agwat.2011.06.007

Mallick, K., Fisher, J. B., Tu, K. P., Boegh, E., & Niyogi, D. (2013). Latent heat flux and canopy conductance based on Penman-Monteith, Priestley-Taylor equation and Bouchet's complementary hypothesis: validation over multiple biomes. *Journal of Hydrometeorology*

Mendina, M., & Terra, R. (2012). Sensitivity of simulated convection to soil moisture in a region in central Amazon. *Atmósfera, Atmósfera vol.25 no.3 México jul. 2012*.

Monteith, J. L. (1965). Evaporation and the environment. In: The state and movement of water in living organisms. *19th Symp. Soc. Biol*, 205 – 234.

NCAP. (2011). Annual Report 2010-11,NATIONAL CENTRE FOR AGRICULTURAL ECONOMICS AND POLICY RESEARCH. [Report]. (NCAP Annual Report 2010-11).

Raju, P. V., Sesha Sai, M. V. R., & Roy, P. S. (2008). In-season time series analysis of Resourcesat-1 AWiFS data for estimating irrigation water requirement. *International Journal of Applied Earth Observation and Geoinformation, 10*(2), 220-228. doi: 10.1016/j.jag.2008.01.004

Ray, S. S., & Dadhwal, V. K. (2001). Estimation of crop evapotranspiration of irrigation command area using remote sensing and GIS. *Agricultural Water Management, 49*(3), 239-249. doi: 10.1016/s0378-3774(00)00147-5

Ray, S. S., Dadhwal, V. K., & Navalgund, R. R. (2002). Performance evaluation of an irrigation command area using remote sensing: a case study of Mahi command, Gujarat, India. *Agricultural Water Management, 56*(2), 81-91. doi: 10.1016/s0378-3774(02)00006-9

Reeling, C. J., Lee, J., Mitchell, P., Halimi, G. H., & Carver, A. (2012). Policy options to enhance agricultural irrigation in Afghanistan: A canal systems approach. *Agricultural Systems, 109*(0), 90-100. doi: 10.1016/j.agsy.2012.03.005

Reichle, R. H., & Koster, R. D. (2004). Bias reduction in short records of satellite soil moisture. *Geophysical Research Letters, 31*(19), n/a-n/a. doi: 10.1029/2004gl020938

Rijtema, P. E. (1965). An analysis of actual evapotranspiration. *Agric. Res Pudoc,Wageningen*

Rep., 659,, 107

Shenbin, C. Y., L; Thomas, A. (2006). Climatic change on the Tibetan Plateau: Potential evapotranspiration trends from 1961-2000. *Climatic Change, 76*(3), 291- 319

Smith, M. (1992). CROPWAT, a computer program for irrigation planning and management *Irrigation and Drainage ,, FAO, Rome, Italy., Paper 46*.

Su, Z. (2001). A Surface Energy Balance System (SEBS) for estimation of turbulant heat fluxes from point to continental scale *In: Advanced Earth Observation-Land surface Climate, Z.Su and Jacobs, C.*

Su, Z. (2002). The Surface Energy Balance System (SEBS) for estimation of turbulent heat fluxes. *Hydrology and Earth System Sciences, 6*(1), 85-99.

Su, Z. (2005). Estimation of the surface energy balance. *In: Encyclopedia of hydrological sciences: 5 Volumes. / ed. by M.G.Anderson and J.J.McDonnell. Chichester eta., Wiley and Sons*(2005), 314p. ISBN:310-471-49103-49109. , 49102, 49731-49752.

Su, Z., Li, X., Zhou, Y., Wan, L., Wen, J., Sintonen, K., & Ieee. (2003). *Estimating areal evaporation from remote sensing*.

Thapa, G., & Gaiha, R. (2011). Smallholder Farming in Asia and the Pacific:Challenges and Opportunities. *Conference on New Directions for Smallholder Agriculture, International Fund for Agricultural Development*

Thornthwaite, C., & Mather, J. (1951). The role of evapotranspiration in climate. *Theoretical and Applied Climatology, 3*(1), 16-39. doi: 10.1007/bf02242588

Timmermans, J., Van Der Tol, C., Verhoef, A., Verhoef, W., Su, Z., Van Helvoirt, M., & Wang, L. (2011). Quantifying the uncertainty in estimates of surface- atmosphere fluxes through joint evaluation of the SEBS and SCOPE models. *Hydrology and Earth System Sciences Discussions, 8*(2), 2861-2893. doi: 10.5194/hessd-8-2861-2011

Timmermans, W. J., Kustas, W. P., Anderson, M. C., & French, A. N. (2007). An intercomparison of the Surface Energy Balance Algorithm for Land (SEBAL) and the Two-Source Energy Balance (TSEB) modeling schemes. *Remote Sensing of Environment, 108*(4), 369-384. doi: 10.1016/j.rse.2006.11.028

van der Tol, C. (2012). Validation of remote sensing of bare soil ground heat flux. *Remote Sensing of Environment, 121*(0), 275-286. doi: http://dx.doi.org/10.1016/j.rse.2012.02.009

van der Tol, C., Verhoef, W., Timmermans, J., Verhoef, A., & Su, Z. (2009). An integrated model of soil-canopy spectral radiances, photosynthesis, fluorescence, temperature and energy balance. *Biogeosciences, 6*(12), 3109-3129.

Verhoef, W., & Bach, H. (2007). Coupled soil–leaf-canopy and atmosphere radiative transfer modeling to simulate hyperspectral multi-angular surface reflectance and TOA radiance data. *Remote Sensing of Environment, 109*(2), 166-182. doi: http://dx.doi.org/10.1016/j.rse.2006.12.013

Verhoef, W., Li, J., Qing, X., & Su, Z. (2007). Unified Optical-Thermal Four-Stream Radiative Transfer Theory for Homogeneous Vegetation Canopies. *Geoscience and Remote Sensing, IEEE Transactions on, 45*(6), 1808-1822. doi: 10.1109/tgrs.2007.895844

Verhoef, W., Xiao, Q., Jia, L., & Su, Z. (2007). Unified optical-thermal four-stream radiative transfer theory for homogeneous vegetation canopies. *IEEE Transactions on Geoscience and Remote Sensing, 45*(6), 1808-1822.

Villagarcía, L., Were, A., Domingo, F., García, M., & Alados-Arboledas, L. (2007). Estimation of soil boundary-layer resistance in sparse semiarid stands for evapotranspiration modelling. *Journal of Hydrology, 342*(1–2), 173-183. doi: http://dx.doi.org/10.1016/j.jhydrol.2007.05.023

Wang, Y. Y., Lia, X., & Ieee. (2011). *SENSIBLE HEAT FLUX ESTIMATION USING SURFACE ENERGY BALANCE SYSTEM (SEBS), MODIS PRODUCTS, AND NCEP REANALYSIS DATA*.

Xiong, J., Wu, B. F., Zhou, Y. M., Li, J., & Ieee. (2006). *Estimating Evapotranspiration using Remote Sensing in the Haihe Basin*.

Yang, S. Q., Sun, R., Mao, D. F., Zhang, X. H., Cu, H. Y., & ieee. (2004). *Estimation of daily evapotranspiration in the Yellow River Basin by using MODIS data*.

Zerihun, D., Wang, Z., Rimal, S., Feyen, J., & Mohan Reddy, J. (1997). Analysis of surface irrigation performance terms and indices. *Agricultural Water Management, 34*(1), 25-46. doi: 10.1016/s0378-3774(97)00005-x

Zwart, S., & Leclert, L. (2010). A remote sensing-based irrigation performance assessment: a case study of the Office du Niger in Mali. *Irrigation Science, 28*(5), 371-385. doi: 10.1007/s00271-009-0199-3

APPENDICES

SEBS THEORY

I. Determination of surface energy balance terms

SEBS uses the energy balance equation to estimate the latent heat flux at the time of overpass (ToP surface energy balance equation states:

$$R_n = G_0 + H + \lambda E \quad 1$$

Where,

R_n is the net radiation [Wm^{-2}]

, G_0 is the ground heat flux [Wm^{-2}]

λE is the latent heat flux [Wm^{-2}]

H is the sensible heat flux [Wm^{-2}]

The net radiation can also be calculated by the following equation:

$$R_n = (1-\alpha)\mathrm{R_{swd}} + \varepsilon.\mathrm{R_{lwd}} - \varepsilon\sigma \mathrm{T}_0^4 \quad 2$$

Where,

α is the broadband surface albedo[-],

R_{swd} and R_{lwd} are the downward shortwave and longwave radiation [W/m^2],

ε is the surface emissivity[-],

σ is the Stefan-Boltzmann's constan[watt m^{-2} K^{-4}]

T_0 is the remotely sensed surface temperature [^0C.]temperature K.

The parameterization of the ground heat flux adopted is as:

$$G_0 = R_n[\Gamma_c + (1-f_c)(\Gamma_s - \Gamma_c)] \quad 3$$

Where ,

Γ_c and Γ_s are the ratio of soil heat flux to net radiation, fixed at 0.05 and 0.315 respectively[-]

f_c is the fractional canopy coverage[-]

II. Determination of aerodynamic roughness height

The aerodynamic roughness height is where the mean wind speed theoretically becomes zero. and is known as the "Aerodynamic Roughness for momentum transport". It is a very important parameter in the energy balance system and is determined by using the equation given in (W.G.M. Bastiaanssen, 1995):

$$Z_{om} = exp(C_1 + C_2 NDVI) \quad 4$$

Where,

C_1=-5.5

C_2=5.8

III. Determination of roughness length for heat transfer

The roughness height for the heat transfer changes with surface characteristics, atmospheric flow and thermal dynamics state of the surface (Su, 2001). SEBS needs a functional form to describe the vertical structure of the vegetation canopy to calculate the within canopy wind speed profile extinction coefficient, n_{ec} and it is derived by the following equation:

$$n_{ec} = -\frac{C_d.LAI}{\frac{2u_*^2}{u(h)^2}} \qquad 5$$

Where,
C_d is the drag coefficient of the foliage elements and is taken as 0.2. [-]
LAI is the one sided leaf area index defined for the total area. [m^2m^{-2}]
U(h) is the horizontal wind speed at the canopy top. [ms^{-1}]

The scalar roughness height for the heat transfer Z_{oh} is given by:

$$Z_{oh} = Z_{om}/exp(kB^{-1}) \qquad 6$$

Where, B^{-1} is a dimensionless heat transfer coefficient and the inverse of Stanton number. It is expressed as:

$$kB^{-1} = \frac{kC_d}{4C_t\frac{u_*}{u(h)}\left(1-e^{-n_{ec}/2}\right)} f_c^2 + 2f_cf_s\frac{k.{}^{u_*}/_{u(h)}.{}^{Z_{om}}/_{h}}{C_t^*} + kB_s^{-1}f_s^2 \qquad 7$$

Where
fc is the fractional canopy coverage [-]
fs is its compliment. [-]
Ct is the heat transfer coefficient of the leaf. [W $m^{-2}K^{-1}$]
C_t^* is the heat transfer coefficient of the soil and is given by: [W $m^{-2}K^{-1}$]

$$C_t^* = Pr^{-2/3}Re_*^{-1/2} \qquad 8$$

Where *Pr* is the Prandtl number and Re_*, the roughness Reynolds number, is expressed by the following equation:

$$Re_* = h_su_*/v \qquad 9$$

Where, *hs* is roughness height of the soil[m], *v* is the kinematic viscosity of the air[ms^{-1}], *p* is a function of ambient pressure[kpa], and *T* temperature[K]. The kinematic viscosity of the air is expressed by the following equation:

$$v = 1.327.10^{-5}(p_0/p)(T/T_0)^{1.81} \qquad 10$$

IV. Determination of sensible heat flux and latent heat flux using similarity theory

In the Atmospheric Surface Layer (ASL), that usually refers to the ten per cent of the bottom of the Atmospheric Boundary Layer (ABL), the similarity relationships for the profiles of the mean wind speed, u, the mean temperature, the difference between the potential temperature at the surface, θ_0 and the potential temperature at height Z, θ_a is expressed in the following equations:

$$u = \frac{u_*}{k}\left[\ln\left(\frac{z-d_0}{z_{om}}\right) - \Psi_m\left(\frac{z-d_0}{L}\right) + \Psi_m\left(\frac{z_{om}}{L}\right)\right] \quad 11$$

$$\theta_0 - \theta_a = \frac{H}{ku_*\rho C_p}\left[\ln\left(\frac{z-d_0}{z_{oh}}\right) - \Psi_h\left(\frac{z-d_0}{L}\right) + \Psi_h\left(\frac{z_{oh}}{L}\right)\right] \quad 12$$

Where, z is the reference/measurement height above the surface[m], u_*, the friction velocity [ms^{-1}]is a function of the surface shear stress and the density of air, k, is the von Karman's constant at 0.4, d_0 is the zero plane displacement height[m], z_{om} is the roughness height for the momentum transfer[m], z_{oh} is the scalar roughness height for heat transfer[m], Ψ_m and Ψ_h are the integrated stability correction functions for momentum and sensible heat transfer respectively, L is the Obukhov length and is expressed as:

$$L = \rho C_p u_*^3 \theta_v / kgH \quad 13$$

Where,
g is the acceleration due to gravity [ms^2]
ms^{-2}] and θ_v is the potential virtual temperature near the surface [K].

Using the Atmospheric Boundary Layer (ABL) similarity (BAS) functions proposed by (Brutsaert, 1999) the system of equations 11,12 and 13 relate, surface fluxes to surface variables and the mixed layers of atmospheric variables. This function is valid for unstable conditions only. For stable conditions the expressions proposed by (Beljaars & Holtslag, 1991) are used for atmospheric surface layer scaling. The friction velocity, the sensible heat flux and the Obukhov stability length are obtained after solving the system of nonlinear equations 11,12 and 13 while derivation of the sensible heat flux using equations 11, 12 and 13 requires only the wind speed and temperature at the reference height as well as the surface temperature and is independent of other surface energy balance terms. This is done via a converging iteration procedure that assumes neutrality as first step. To determine the sensible heat SEBS uses the limiting cases in the energy balance equation. Under dry limits the latent heat becomes zero due to the limitation of soil moisture and the sensible heat flux is at the maximum value and the process is shown in the following equations:

$$\lambda E_{dry} = R_n - G_0 - H_{dry} = 0 \quad , \quad H_{dry} = R_n - G_0 \quad 14$$

Under wet limit, where the evaporation takes place at the potential rate, the sensible heat flux is at its minimum values.

$$\lambda E_{wet} = R_n - G_0 - H_{wet} \quad , \quad H_{wet} = R_n - G_0 - \lambda E_{wet} \quad 15$$

The relative evaporation is evaluated as:

$$\Lambda_r = \frac{\lambda E}{\lambda E_{wet}} = 1 - \frac{\lambda E_{wet} - \lambda E}{\lambda E_{wet}} \quad 16$$

Using equation 1, 14, 15 and 16 the relative evaporative fraction is expressed in terms of sensible heat and the limiting cases as

$$\Lambda_r = 1 - \frac{H - H_{wet}}{H_{dry} - H_{wet}} \quad 17$$

Where,
H is the actual sensible heat.
H_{wet} can be obtained by combining equations 15 with Penman-Monteith (Monteith, 1965) and is expressed as follows:

$$\lambda E = \frac{\Delta . r_e(R_n - G_0) + \rho C_p . (e_{sat} - e)}{r_e(\gamma + \Delta) + \gamma . r_i} \qquad 18$$

Where e and e_{sat} are actual and saturated vapour pressure respectively [Pa], γ is the psychometric constant [PaK^{-1}] and Δ rate of change of saturation vapour pressure with temperature [PaC^{-1}], r_i is the bulk surface internal resistance and r_e is the external or aerodynamic resistance [sm^{-1}]. At wet limit, the internal resistance r_i=0. This equation stands valid for a soil surface as well as a vegetated canopy with properly defined bulk internal resistance. Using this property in equation 18 the sensible heat flux at the wet limit is obtained as:

$$H_{wet} = \frac{\left[(R_n - G_0) - \frac{\rho C_p}{r_{ew}} . \frac{e_s - e}{\gamma}\right]}{\left[1 + \frac{\Delta}{\gamma}\right]} \qquad 19$$

The external resistance at wet limit can be determined by the following equation:

$$r_{ew} = \frac{1}{k u_*}\left[\ln\left(\frac{z - d_0}{z_{oh}}\right) - \Psi_h\left(\frac{z - d_0}{L_w}\right) + \Psi_h\left(\frac{z_{oh}}{L_w}\right)\right] \qquad 20$$

The stability length L_w, at wet limit, is determined by:

$$L_w = -\frac{\rho u_*^3}{kg . 0.61 . (R_n - G_0)/\lambda} \qquad 21$$

The evaporated fraction is expressed as follows:

$$\Lambda = \frac{\lambda E}{R_n - G} = \frac{\Lambda_r . \lambda E_{wet}}{R_n - G} \qquad 22$$

Up- scaling of daily ET
To up –scaling of evaporative fraction to daily ET values, the evaporative fraction is assumed constant during the day, so the following equitation was used:

$$E_{daily} = 8.64 * 10^7 * \overset{24}{\underset{0}{\Lambda}} * \frac{\overline{R_n} - \overline{G_o}}{\lambda \rho w} \qquad 23$$

Where E_{daily} is the daily actual ET in [mm day^{-1}].